Taxonomic and Functional Alterations in the Gut Microbiome of Patients with Lewy Body Dementia and Their Cohabitant Controls

A Thesis
Submitted to the Faculty of the Graduate School
of the University of Minnesota
by

Xiaowei Zhao

In Partial Fulfillment of the Requirements
For the Degree of
Master of Science

Advisor: Jaeyun Sung, Ph.D.

December 2025

Acknowledgements

I would like to express my deepest appreciation to my advisor, Dr. Jaeyun Sung, for his continuous guidance, encouragement, and support. I am truly grateful that he gave me the opportunity to begin my bioinformatics journey and start building my career in this field. With his mentorship, I was able to study and work at the Mayo Clinic, where I had the chance to collaborate with many clinicians and researchers and learn from their expertise. I also deeply appreciate the opportunity to work as a bioinformatics intern under his supervision, which allowed me to gain valuable hands-on experience with real clinical data through various microbiome and proteomics projects. All these experiences that Dr. Sung has provided will always be deeply appreciated and remembered throughout my life.

I would also like to express my sincere gratitude to the Bioinformatics and Computational Biology (BICB) Graduate Program at the University of Minnesota for providing such a supportive and inspiring environment for students' education. I am especially thankful to Dr. Yuk Sham, Dr. Chad Myers, and Miranda Nelson for their dedication to the program and their constant care for its students. Their efforts in organizing symposiums, seminars, and other events have greatly enriched our learning experience, and their willingness to listen and help us whenever we face challenges has been truly encouraging. I am very grateful for all their support and proud to be part of the BICB community.

I cannot say enough to express my gratitude to all the current and previous members of Dr. Sung's lab, including Dr. Vinod Gupta, Dr. Benjimin Hur, Adam Koller,

Thomas Pelowitz, Maria Barrera-Suarez, Dr. Conan Zhao, and Kevin Cunningham. Being part of such a collaborative and supportive lab has given me many opportunities to learn from my seniors and peers about their projects and skillsets. As a beginner in computational biology, I relied a lot on the knowledge and technical help from everyone in the lab when I first started, and I truly appreciate all their patience and guidance. Specifically, I would like to thank Dr. Vinod Gupta and Dr. Benjimin Hur. They are not only my closest colleagues but also my best friends in life. Their knowledge and skillsets are exceptional, and I have learned so much simply by talking with them and observing their daily work. Their attitude toward research and science truly inspires me to stay curious and keep learning new knowledge. Their guidance and encouragement have always given me strength and confidence, especially when I faced obstacles or challenges. Their integrity and honesty are qualities I truly admire and will always look up to. The laughter and tears we shared together are one of the most meaningful and unforgettable memories in my life.

My research project would not have been possible without our amazing and hardworking collaborators. I would like to thank Dr. Stuart McCarter, Dr. Levi Teigen, and their dedicated teams for recruiting patients and collecting stool samples. I am also very grateful for their deep expertise and valuable feedback, which greatly helped me during my thesis writing. In addition, I would like to thank my committee members, Dr. Christopher Staley and Dr. Helen Vuong, for their thoughtful advice and constructive suggestions on my research.

Last but certainly not least, I want to thank my family and friends for their endless love and support. My dear husband, Weiguo Han, has always stood by my side with unconditional understanding and care. He listened patiently whenever I felt stressed or frustrated, and his love and humor brought so much joy into my life. Being with him is truly the happiest and most relaxing place I can be. I am also deeply grateful to my parents for their constant encouragement and love. Even though they may not fully understand my research, they have always been proud of me and willing to listen, which means the world to me. I also want to thank my dear friends, Michelle Bland, Janet Yao, Alberta Marana, Mick McDonnell, Roger Mehling, and Julie Kim, for bringing so much laughter, warmth, and happiness into my graduate school life. Their kindness, support, and the way they cared for me like family made this journey so much brighter and more memorable.

Dedication

This thesis is dedicated to my beloved husband and parents for their unconditional love and support.

Abstract

Lewy body dementia (LBD) is a progressive α-synucleinopathy and the second most common type of dementia after Alzheimer's disease. Idiopathic rapid eye movement (REM) sleep behavior disorder (iRBD) represents a prodromal stage of LBD. Increasing evidence has shown the important role of the gut microbiome and the gut-brain axis in various neurodegenerative diseases, including Alzheimer's disease and Parkinson's disease. However, how gut microbial alterations contribute to the progression from iRBD to LBD remains largely unknown.

In this study, we analyzed stool samples from 25 LBD patients, 10 iRBD patients, and their cohabitant controls using shotgun metagenomic sequencing to comprehensively profile microbial taxonomy and metabolic functions. From the sequencing data, taxonomic and functional features were characterized using the MetaPhlAn4 and HUMAnN3 computational pipelines. Afterwards, statistical analyses, such as mixed-effects linear regression models and Fisher's exact tests, were applied to identify differentially abundant and prevalent microbial species and pathways. Correlation analyses were further performed to explore associations between microbial features and clinical measures of cognition and motor function, mainly Clinical Dementia Rating-Sum of Boxes (CDR-SB), Montreal Cognitive Assessment (MoCA), Short Test of Mental Status (STMS), and Movement Disorder Society-Unified Parkinson's Disease Rating Scale Part III (MDS-UPDRS III).

Although overall microbial α-diversity and β-diversity did not differ significantly between patients and their cohabitant controls, specific microbial taxa and metabolic

pathways showed clear alterations in both LBD and iRBD. The abundance of *Hungatella hathewayi* and *Collinsella aerofaciens* were significantly higher in LBD and iRBD, respectively, while beneficial short-chain fatty acid-producing bacteria such as *Eubacterium ramulus* and *Roseburia hominis* had lower abundance in LBD, along with less *Bacteroides* in both LBD and iRBD compared with their cohabitants. Based on metagenomic functional profiling, we observed several lower abundances of metabolic functions in LBD and/or iRBD. For example, the starch degradation III pathway was lower in LBD, and the L-histidine degradation III pathway was lower in both LBD and iRBD, suggesting less microbial potential for short-chain fatty acid and GABA production. In contrast, pathways involved in lipopolysaccharide biosynthesis, such as ADP-L-glycero-β-D-manno-heptose biosynthesis and O-antigen building block biosynthesis, had higher abundance, indicating enhanced pro-inflammatory potential. Correlation analyses further revealed that *Christensenella hongkongensis* abundance was negatively correlated with cognitive impairment and dementia severity in LBD patients, while *Clostridium leptum* and *Coprococcus comes* showed the same negative associations in iRBD patients. Likewise, in LBD, the superpathway of L-alanine biosynthesis and the Bifidobacterium shunt were both positively correlated with cognitive and motor performance. In iRBD, higher abundance of the myo-, chiro-, and scyllo-inositol degradation pathway correlated with better cognitive and motor function.

Together, these findings demonstrate both shared and stage-specific taxonomic and functional alterations in the gut microbiome along the LBD disease continuum. Our results highlight potential metabolic functions involving short chain fatty acids (SCFAs),

neurotransmitter, and endotoxin metabolism that may influence neuroinflammation, gut barrier integrity, and neuronal signaling, highlighting the role of gut-brain interactions in LBD disease continuum.

Table of Contents

List of Tables

List of Figures

Introduction

Lewy body dementia (LBD) is a progressive neurodegenerative disorder and a major α-synucleinopathy. It is the second most common type of dementia after Alzheimer's disease, accounting for up to 15% of all cases of dementia in the United States[1,2]. Pathologically, it is characterized by the accumulation of misfolded α-synuclein proteins into Lewy bodies in neurons in the cerebral cortex, limbic cortex, hippocampus, midbrain and basal ganglia, and brain stem[3,4]. These proteins can damage neurons and disrupt synaptic and neuronal functions, which cause problems with sleep, cognitive, mood, behavior, and movement[5-8]. Patients are typically diagnosed with LBD when cognitive impairment, such as memory or attention problems, appears before or within one year of developing movement symptoms[8]. Clinically, LBD presents a broad range of symptoms including progressive cognitive decline, fluctuations in attention, recurrent visual hallucinations, autonomic dysfunction, parkinsonism, and REM sleep behavior disorder (RBD)[8-10]. Although these clinical features are not always present in every patient, when they do occur, they are highly specific and strongly indicative of underlying Lewy body pathology[11].

REM sleep behavior disorder (RBD) is a parasomnia characterized by loss of normal muscle atonia during REM sleep, where people physically act out their dreams such as vocalizations or complex motor activity[12]. It is a male-predominant disorder that typically appears in individuals over 50 years of age[13]. The idiopathic form of this disorder (iRBD) is diagnosed when dream-enactment behaviors are confirmed by both history and polysomnography, and no presence of any other associated neurological disorders or

other possible causes[14]. RBD may also occur as a secondary form in individuals with other underlying conditions or following the use of certain medications[12]. The main mechanistic cause of RBD is believed to be a dysfunction of the neural circuit that switches between sleep states, caused by an imbalance between excitatory and inhibitory neuronal populations that regulate REM and non-REM transitions[15]. Disruption of this circuit can lead to REM sleep without atonia, which is a key feature in the pathophysiology of iRBD, where the absence of muscle atonia results in dream enactment behaviors[13,15,16].

RBD is frequently observed in neurodegenerative disorders, particularly in α-synucleinopathies[17]. Studies have shown that in α-synucleinopathies, neuronal loss commonly occurs within brainstem structures that regulate REM muscle atonia[18,19]. Autopsy findings in iRBD patients have demonstrated widespread Lewy body pathology, particularly in brainstem and limbic regions[20]. Longitudinal cohort studies have further shown that over 90% of iRBD patients eventually develop neurodegenerative diseases during long-term follow-up, with approximately one in four devolping LBD[21]. Among LBD patients who have RBD, 71–100% experience RBD symptoms before the onset of cognitive decline and dementia typically follows about 6–10 years later[22-26]. Therefore, RBD is considered a strong prodromal marker and an early indicator of α-synucleinopathies[27,28], especially LBD[29]. This close clinical and pathological relationship between iRBD and LBD supports the concept that they represent a disease continuum[12]. Studying both conditions within this continuum provides a valuable opportunity to

investigate disease mechanisms years before dementia develops and to identify early biomarkers or therapeutic targets.

The gut-brain axis is a bidirectional communication system between the central nervous system (CNS) and the gastrointestinal (GI) tract[30,31]. It integrates immune signaling, vagal and enteric neural pathways, endocrine routes, and microbiota-derived metabolites and neurotransmitters[32-34]. Growing evidence suggests that this system plays a critical role in disease pathogenesis, with the gut microbiome increasingly implicated across neurological disorders[32,35]. Associations have been reported in Alzheimer's disease[36,37], autism spectrum disorder[38,39], depression and anxiety[40,41], and others[42]. Moreover, multiple studies of α-synucleinopathies such as Parkinson's disease (PD) have consistently demonstrated a decreased abundance of short-chain fatty acid-producing bacteria and an increased prevalence of pro-inflammatory taxa[43-46].

Despite growing evidence for the role of the gut-brain axis in various neurological disorders, relatively few studies have specifically examined the gut microbiome in LBD. Nishiwaki et al. analyzed stool samples using 16S rRNA sequencing from 28 patients with dementia with Lewy bodies (DLB), 26 patients with iRBD, and 147 controls[47]. They reported a decreased abundance in short-chain fatty acid-producing bacteria, along with increased abundance of *Ruminococcus torques* and *Collinsella* in DLB compared with controls. More recently, Teigen *et al.* investigated 27 LBD patients, 11 iRBD patients, and their cohabitant household controls to account for shared environmental and dietary factors[48]. They observed no major differences in overall microbiome diversity or

composition between patients and cohabitants; however, the iRBD group showed a notably lower abundance of *Bacteroides*.

Most gut microbiome studies in neurodegenerative diseases, including LBD, have used the 16S rRNA sequencing technique. The 16S rRNA gene serves only as a phylogenetic marker and is not directly involved in metabolic functions. Consequently, 16S sequencing can provide only indirect functional inferences by linking identified taxa to limited known capabilities in reference database[49]. This approach cannot fully capture the functional impact of the microbiome on disease pathology. Therefore, functional profiling of the microbiome using shotgun metagenomic sequencing can provide deeper insight by looking at the microbial metabolic pathways and gene families encoded within the community[50]. This level of analysis is important because microbial metabolism generates a wide range of compounds, such as short-chain fatty acids, bile acids, and neurotransmitters or their precursors, that can modulate host immune responses, intestinal barrier integrity, and neural signaling pathways[51-53]. Through these mechanisms, microbial metabolic activity can influence multiple host systems relevant to neurodegeneration, including neuroinflammation and oxidative stress[53,54]. The increase or depletion of these products therefore provides a mechanistic window into how the gut microbiome might accelerate or mitigate disease progression in LBD.

In microbiome research, a high degree of inter-individual variation is commonly observed[55,56]. Such variability largely reflects differences in host genetics and environmental factors, including diet, lifestyle, and medication use[57-59]. A previous study comparing genetically unrelated children living in the same household with genetically

related children raised in different households found that a shared home environment was the strongest predictor of overall gut microbiome similarity[60], which indicates that living environment can have a greater influence on the gut microbiome than host genetics. Studies have also shown that individuals living in the same household share more similar microbiota than those from different homes, highlighting the influence of cohabitation on the gut microbiome structure[59-61]. Therefore, including cohabitant controls in microbiome studies helps reduce background variability caused by differences in environment and diet and allows better detection of disease-associated microbial changes.

In this study, we recruited patients with LBD and iRBD together with their cohabitant controls to investigate differences in gut microbiome composition and function. We assessed differences in microbiome diversity, taxonomic composition, and metabolic potential between LBD, iRBD, and controls, and further examined associations between microbial features and clinical measures of cognition and motor function. Through this approach, we aimed to identify microbial taxa and pathways that may contribute to LBD or iRBD pathology. Our major goal is to provide new insights into the role of the gut–brain axis in LBD, highlight potential microbial biomarkers of disease progression and suggest avenues for early mechanistic understanding and therapeutic intervention.

Methods

Participant enrollment

Participant enrollment followed procedures described in our previous work[48]. Briefly, this study was approved by the Mayo Clinic Institutional Review Board (IRB: 18-011778), and informed consent was obtained from all participants. Participants were recruited from the Mayo Clinic Alzheimer's Disease Research Center and the North American Prodromal Synucleinopathy (NAPS) cohort. The study population included 25 patients with LBD who met research criteria for prodromal DLB (n = 10) or DLB (n = 15), 10 polysomnographically proven patients with iRBD, and their cohabitant controls. All patients underwent comprehensive clinical interview, neurologic examination and neuropsychological testing by sleep/behavioral neurology subspecialty neurologists and neuropsychologists. Following evaluation, a consensus clinical diagnosis of MCI-LB, DLB or iRBD was made based on established clinical criteria. Since consensus diagnostic criteria for iRBD are not established, iRBD was defined as the presence of normal neuropsychological testing with absence of parkinsonism. Demographic and clinical information was collected for all participants, including age, sex, dementia severity (Clinical Dementia Rating [CDR] global and sum of boxes [SB]), bedside cognitive testing score (Kokmen Short Test of Mental Status [STMS], Montreal Cognitive Assessment [MoCA] and parkinsonism severity (Movement Disorders Society-Unified Parkinson's Disease Rating Scale Part III [MDS-UPDRS III]).

Stool sample collection, DNA extraction, and shotgun metagenome sequencing

Fecal samples were collected using standard stool specimen collection kits at the time of clinical assessment. All samples were transferred to the University of Minnesota Genomics Center for DNA extraction and sequencing. Fecal DNA was extracted using the DNeasy 96 PowerSoil Pro QIAcube HT Kit (QIAGEN, Germantown, MD, USA) according to the manufacturer's instructions. DNA concentration was assessed using both a NanoDrop-8000 UV-Vis spectrophotometer (ThermoScientific, Wilmington, DE, USA) and PicoGreen assays. Extraction was automated using the QIAcube platform with the inhibitor removal technology (IRT) protocol. Libraries were sequenced on an Illumina NovaSeq 6000 using 2×150 bp paired-end chemistry, targeting 8 million paired-end reads per sample. Sequencing data for stool metagenomes used in this study have been deposited at NCBI's Sequence Read Archive (SRA) data repository (PRJNA1368951).

Quality filtration of sequenced reads

Metagenomic reads were processed using an in-house quality control pipeline. Specifically, Trimmomatic v0.39[62] was used to remove adapter and overrepresented sequences (ILLUMINACLIP: adaptor_overrepresented.fa:2:30:10:2:keepBothReads), trim low-quality bases from the start and end of reads (LEADING:3 and TRAILING:3), and discard reads shorter than 60 bp (MINLEN:60). Host-derived reads were subsequently removed by aligning to the Human Genome Reference Database (GRCh38) using Bowtie2 v2.5.0[63], followed by filtering with SAMtools v1.18[64].

Taxonomic and functional profiling of stool metagenomes

Taxonomic profiling was performed using the MetaPhlAn4 v4.1.15[65] phylogenetic clade identification pipeline with default parameters. Briefly, MetaPhlAn4 identifies microbial taxonomy and composition by detecting unique clade-specific marker genes. The marker database (mpa_vJun23_CHOCOPhlAnSGB_202403) is derived from a curated collection of 1.01 M prokaryotic reference and metagenome-assembled genomes, encompassing 26,970 species-level genome bins, 4,992 of which are taxonomically unidentified at the species level. Microbial taxa of viral origin and those labeled as unclassified or unknown were excluded from further analyses. Microbiome profiles were then normalized using total sum scaling (TSS) to obtain the relative abundances of microbial taxa.

Functional profiling of microbial communities was conducted using HUMAnN3 v3.96[66] with default parameters. Briefly, HUMAnN3 first maps quality-controlled metagenomic reads to species-specific pangenomes to quantify gene families and subsequently aligns unmapped reads to the UniRef90 database to improve detection sensitivity. Gene family abundances are then used to reconstruct microbial metabolic pathways based on the MetaCyc database. Pathways classified as unmapped (i.e., reads that did not align to any gene family) or unintegrated (i.e., gene families not assigned to any known pathway) were excluded from downstream analyses. The relative abundances of the remaining pathways were normalized using TSS via the “humann_renorm_table --units relab --special n” utility in HUMAnN3. In parallel, the relative abundances of gene families were also characterized for downstream analyses.

Gut microbiome diversity analysis

Overall gut microbiome composition was evaluated by calculating both α-diversity (species-level Shannon index and richness) and β-diversity (Bray–Curtis distances between all sample pairs). The R package "vegan" v2.6-10 was used to calculate Shannon index and species richness based on untransformed relative abundances of microbial species in each stool metagenome. To compare α-diversity between LBD/iRBD patients and their cohabitant controls, mixed-effects linear regression models were constructed using the R packages "lmerTest" v3.1-3 and "lme4" v1.1-37, with household ID included as a random effect. For comparisons between LBD and iRBD patients, simple linear model without random effects was used. *P*-values less than 0.05 were considered statistically significant. For β-diversity analysis, principal coordinate analysis (PCoA) was performed using Bray–Curtis dissimilarities calculated on arcsine square-root transformed relative abundances of microbial species identified by MetaPhlAn4. This analysis was implemented using the R packages "ade4" v1.7-23 and "vegan" v2.6-10.

PERMANOVA on taxonomic composition of microbial communities

A permutational multivariate analysis of variance (PERMANOVA) was conducted on the Bray–Curtis dissimilarity matrix using the "adonis2" function from the R package "vegan". *P*-values for the pseudo-F statistic were calculated based on 999 permutations to assess the proportion of variance in gut microbial community composition explained by disease status and patient characteristics such as age, sex, and BMI. For comparisons between LBD/iRBD patients and their cohabitant controls, permutations were constrained within

households using the strata option to account for paired study design. No permutation constraints were applied for comparisons between LBD and iRBD patients. The output from PERMANOVA was used to estimate the percentage of variance in microbiome composition attributable to disease status and its statistical significance. *P*-values less than 0.05 were considered statistically significant.

Differential abundance and prevalence analysis

Microbial taxonomic and functional features (species, pathways, and gene families) were preprocessed using two filtering steps prior to differential analysis. First, to reduce the influence of extremely low-abundance features that may represent noise or technical artifacts, relative abundance values below a predefined threshold were set to zero based on rank-abundance plots. Specifically, a threshold of $10^{-4.5}$ was applied for taxa and pathways, and 10^{-7} for gene families. Second, to address data sparsity, only features present in at least 10% of samples within each comparison group were selected for downstream differential analysis. Mixed-effects linear regression models were applied to arcsine square-root transformed relative abundance data to identify differentially abundant features (species, pathways, and gene families) between LBD/iRBD patients and their cohabitant controls. The models included age and BMI as fixed effects and household ID as a random effect. These analyses were performed using the R packages "lme4" v1.1-37 and "lmerTest" v3.1-3. To identify differentially abundant features between LBD and iRBD patients, simple linear regression models were used with age and BMI as covariates, without any random effects. Differentially prevalent microbial features were

identified using Fisher's exact test. *P*-values less than 0.05 were considered statistically significant.

Correlations between clinical characteristics and microbial features

To reduce sparsity and improve the robustness of the analysis, microbial taxonomic and functional features were included in the correlation analysis only if they were present in at least 40% of samples within the LBD group and 80% of samples within the iRBD group. Spearman's rank correlation coefficients (ρ) were calculated in R (using the "cor.test" function) between the untransformed relative abundances of filtered microbial features and four clinical measures: three cognitive scores (CDR-SB, MoCA, STMS) and one motor score (MDS-UPDRS III). Correlations with $P < 0.05$ and Spearman's $|\rho| > 0.35$ were considered significant and reported.

Results

Participant demographics

This study includes stool samples from Participant demographic and clinical characteristics are shown in **Table 1**. LBD patients ranged in age from 46 to 73 years (median = 68), and iRBD patients from 56 to 76 years (median = 68). Both groups were slightly older than their cohabitant controls; however, the differences were not statistically significant (P = 0.099 and 0.149, respectively; Wilcoxon rank-sum test). Male sex accounted for 84% and 90% of LBD and iRBD patients, respectively, indicating a strong male predominance in both groups ($P \leq 0.001$ for both; Fisher's exact test).

Table 1. Demographic and clinical characteristics of the study population.

Patient characteristics	LBD[a]			iRBD[b]		
	Patients (*n* = 25)	**Household controls (*n* = 25)**	***P*-value[#]**	**Patients (*n* = 10)**	**Household controls (*n* = 10)**	***P*-value[#]**
Age						
Median [Q1, Q3][c]	68.0 [64.0, 73.0]	64.0 [59.0, 71.0]	0.099	68.0 [63.5, 69.8]	63.0 [57.5, 65.5]	0.149
Sex						
Female, *n* (%)	4 (16)	23 (92)	< 0.001	1 (10)	9 (90)	0.001
Male, *n* (%)	21 (84)	2 (8)		9 (90)	1 (10)	
BMI						
Median [Q1, Q3]	26.4 [25.1, 31.2]	26.6 [25.1, 29.3]	0.288	28.9 [26.9, 29.4]	27.5 [24.2, 29.5]	0.533
Not available	2	10		0	3	
Global CDR[d], *n* (%)						
0	0 (0)			5 (50)		
0.5	16 (64)			5 (50)		
1	8 (32)	N/A		0 (0)	N/A	
2	0 (0)			0 (0)		
3	1 (4)			0 (0)		
CDR-SB[e], *n* (%)						
0	0 (0)			5 (50)		
0.5–4.0	15 (60)			5 (50)		
4.5–9.0	9 (36)	N/A		0 (0)	N/A	
9.5–15.5	0			0 (0)		
16.0–18.0	1 (4)			0 (0)		
MDS-UPDRS III[f]						
Median [Q1, Q3]	19.0 [1.0, 26.0]	N/A		0.0 [0.0, 2.5]	N/A	

MoCA[g]				
Median [Q1, Q3]	21.0 [16.8, 27.3]	N/A	25.5 [25.0, 28.5]	N/A
Not available	1		0	
STMS[h]				
Median [Q1, Q3]	31.0 [27.0, 34.0]	N/A	36.5 [36.0, 37.8]	N/A
Visual hallucinations, *n* (%)	9 (36)	N/A	0 (0)	N/A
Cognitive fluctuations, *n* (%)	10 (40)	N/A	0 (0)	N/A
Parkinsonism, *n* (%)	18 (72)	N/A	1 (10)	N/A
REM sleep behavior disorder, *n* (%)	24 (96)	N/A	10 (100)	N/A
Antibiotic use in the last 6 months				
n (%)	8 (32)	4 (16)	1 (4)	2 (8)
Not available	4	2	1	1
Constipation in the last 6 months				
n (%)	20 (80)	N/A	5 (50)	N/A
Not available	1		0	

[a]LBD, Lewy Body Dementia; [b]iRBD, idiopathic Rapid-eye-movement sleep Behavior Disorder; [c]Upper and lower quartiles; [d]Global CDR, Global Clinical Dementia Rating; [e]CDR-SB, Clinical Dementia Rating Scale Sum of Boxes; [f]MDS-UPDRS III, Movement Disorder Society-Unified Parkinson's Disease Rating Scale Part III score; [g]MoCA, Montreal Cognitive Assessment test score; [h]STMS, Short Test of Mental Status score; [#]Mann-Whitney *U* test and Fisher's exact test was used to test for the statistical significance of age and sex, respectively; and mixed-effects linear regression was used to control for household while testing for the statistical significance of BMI; N/A, not applicable or not available.

Overall comparisons of gut microbiome communities

Species-level Shannon index and richness did not differ significantly between LBD/iRBD patients and their cohabitant controls, nor between LBD and iRBD patients (**Figures 1B–C**). This suggests that overall microbial α-diversity at the species level remains largely unchanged across disease and control groups. For β-diversity, PERMANOVA analysis showed that disease diagnosis explained only 2.2%, 5.3%, and 4.1% of the total variance in gut microbial community composition between LBD/iRBD patients and their cohabitant controls, as well as between LBD and iRBD patients, respectively; however, no significant association was found between gut microbial community composition and disease group in any of the three comparisons (P = 0.067, 0.156, and 0.059; **Figures 1D–F**).

We also performed PERMANOVA to evaluate other patient characteristics that might contribute to variance in gut microbial communities of LBD and iRBD patients compared with their cohabitant controls. In univariate models, age, sex, and BMI explained 2.2%, 2.0%, and 2.6% of the total variance in gut microbial communities of LBD patients and their cohabitants, and 5.0%, 4.7%, and 5.3% in those of iRBD patients and their cohabitants (**Table 2**). However, none of these associations were statistically significant (**Table 2**).

The relative abundance of microbial families in gut microbiomes of individuals in LBD/iRBD and their cohabitant controls were shown in **Figures 1G–H**. All families with less than 5% relative abundance or unclassified taxa were grouped into “Others”. Exclude “Others” category, Lachnospiraceae was the most abundant family in all 4 groups (LBD, LBD controls, iRBD, and iRBD controls) in general (median of relative abundance = 0.304,

0.312, 0.273, 0.307, respectively). Oscillospiraceae and Bacteroidaceae were also abundant across all groups. The median relative abundance of Oscillospiraceae was 0.160, 0.168, 0.181, and 0.232 in the LBD, LBD controls, iRBD, and iRBD controls, respectively, while Bacteroidaceae had median values of 0.050, 0.087, 0.000, and 0.085 in the same groups. Some families, such as Akkermansiaceae and Bifidobacteriaceae, were present in high abundance in some individuals but absent in others. Overall, the microbial profiles at the family level indicates clear inter-individual heterogeneity.

Table 2. Patient characteristics contributing to the variance in gut microbial community composition.

	Patient characteristics	**Variance (%)**	***P*-value**
LBD	Disease status	2.2	0.060
	Age	2.2	0.076
	Sex	2.0	0.114
	BMI	2.6	0.235
iRBD	Disease status	5.3	0.156
	Age	5.0	0.567
	Sex	4.7	0.339
	BMI	5.3	0.378

Gut microbiome samples of 25 LBD patients, 10 iRBD patients, and their cohabitant controls were analyzed simultaneously using Permutational Multivariate Analysis of Variance (PERMANOVA); PERMANOVA was used to test for statistical association between corresponding patient characteristic and variance within microbiome composition.

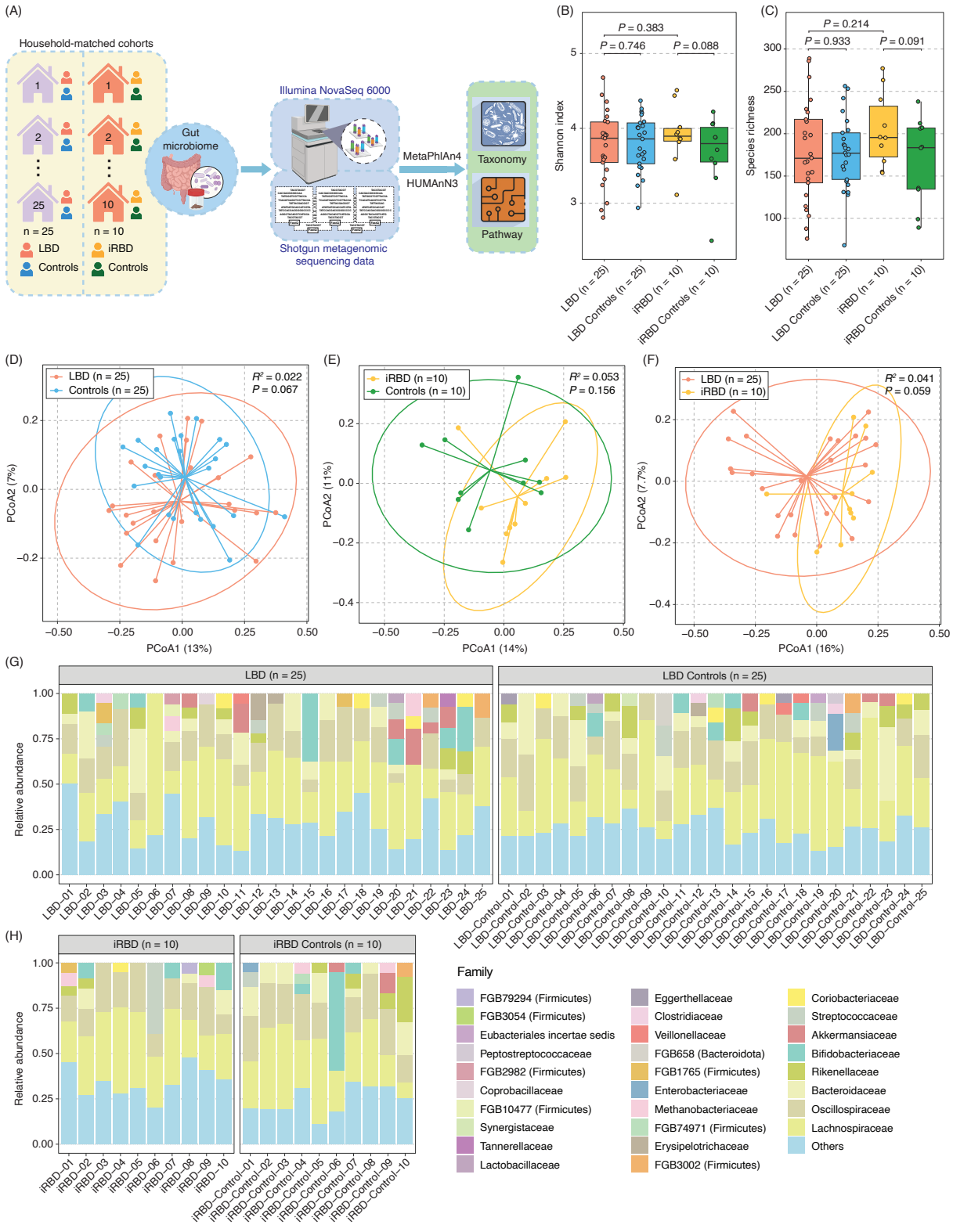
(A)
Household-matched cohorts
n = 25
LBD
Controls
n = 10
iRBD
Controls
Gut microbiome
Illumina NovaSeq 6000
Shotgun metagenomic sequencing data
MetaPhlAn4
HUMAnN3
Taxonomy
Pathway
(B)
Shannon index
P = 0.383
P = 0.746
P = 0.088
LBD (n = 25)
LBD Controls (n = 25)
iRBD (n = 10)
iRBD Controls (n = 10)
(C)
Species richness
P = 0.214
P = 0.933
P = 0.091
(D)
LBD (n = 25)
Controls (n = 25)
R² = 0.022
P = 0.067
PCoA1 (13%)
PCoA2 (7%)
(E)
iRBD (n =10)
Controls (n = 10)
R² = 0.053
P = 0.156
PCoA1 (14%)
PCoA2 (11%)
(F)
LBD (n = 25)
iRBD (n = 10)
R² = 0.041
P = 0.059
PCoA1 (16%)
PCoA2 (7.7%)
(G)
LBD (n = 25)
LBD Controls (n = 25)
Relative abundance
(H)
iRBD (n = 10)
iRBD Controls (n = 10)
Relative abundance
Family
FGB79294 (Firmicutes)
FGB3054 (Firmicutes)
Eubacteriales incertae sedis
Peptostreptococcaceae
FGB2982 (Firmicutes)
Coprobacillaceae
FGB10477 (Firmicutes)
Synergistaceae
Tannerellaceae
Lactobacillaceae
Eggerthellaceae
Clostridiaceae
Veillonellaceae
FGB658 (Bacteroidota)
FGB1765 (Firmicutes)
Enterobacteriaceae
Methanobacteriaceae
FGB74971 (Firmicutes)
Erysipelotrichaceae
FGB3002 (Firmicutes)
Coriobacteriaceae
Streptococcaceae
Akkermansiaceae
Bifidobacteriaceae
Rikenellaceae
Bacteroidaceae
Oscillospiraceae
Lachnospiraceae
Others

Figure 1. Study design and gut microbiome community comparisons.

(A) Stool samples were collected from patients with LBD (n = 25), iRBD (n = 10), and their cohabitant controls. Whole-metagenome shotgun sequencing was performed on all samples using the Illumina NovaSeq 6000 platform. Microbial taxonomic and functional profiling were conducted using MetaPhlAn4 and HUMAnN3, respectively. **(B–C)** No significant differences in species-level Shannon index or richness were observed between patient and control groups, or between LBD and iRBD. Statistical comparisons between patients and controls were performed using mixed-effects linear regression models with household ID as a random effect (to account for intra-household correlation), or simple (i.e., fixed-effect) linear model for comparisons between LBD and iRBD. **(D–F)** PCoA ordination plots based on Bray–Curtis dissimilarity showed no clear separation by disease status, and PERMANOVA tests indicated that disease diagnosis explained minimal variation in overall microbial composition. **(G–H)** Stacked bar plots show the relative abundances of microbial families across LBD, iRBD, and controls. All families with less than 5% relative abundance or unclassified taxa were grouped into "Others". Lachnospiraceae was the most abundant family in most of groups. PCoA, principal coordinates analysis; PERMANOVA, permutational multivariate analysis of variance.

Differential abundance and prevalence between LBD and cohabitant controls

Although no significant differences in α- and β-diversity were observed among LBD, iRBD, and their cohabitant controls, species-level analysis revealed distinct differences in microbial composition between groups. Filtering with the prevalence cut-off (described in the "Methods") yielded a total of 479 microbial species and 433 metabolic pathways for downstream differential analyses. Using a mixed-effects linear regression model adjusted for age and BMI, with household ID as a random effect, we identified significant differences in both microbial species and metabolic pathway relative abundances between LBD patients and their cohabitant controls. In total, four species were significantly more abundant in LBD, while nine were elevated in controls (all $P < 0.05$; **Figure 2A**). Microbial species that were more abundant in LBD included Oscillospiraceae bacterium CLA-AA-H250, *Dorea* sp. AF36-15AT, GGB9522 SGB14921 (Firmicutes), and *Hungatella hathewayi*. In contrast, *Eubacterium rectale*, GGB9480 SGB14874

(Firmicutes), *Roseburia hominis*, *Eubacterium ramulus*, and GGB9760 SGB15373 (Firmicutes) were more abundant in controls (**Figure 3A**). Applying the same model to microbial metabolic pathways uncovered four pathways with significantly higher relative abundance in LBD and six pathways elevated in controls (all $P < 0.05$; **Figure 2B**). Pathways enriched in LBD included L-glutamine biosynthesis III, Superpathway of L-methionine biosynthesis (by sulfhydrylation), ADP-L-glycero-β–D-manno–heptose biosynthesis, and Heme b biosynthesis I (aerobic). In contrast, pathways enriched in the control group included Starch degradation III, β-(1,4)-mannan degradation, L-glutamate and L-glutamine biosynthesis, L-histidine degradation III, and Purine nucleobases degradation II (anaerobic) (**Figure 3B**). The upper panels of **Figures 3A–B** show the mean differences in relative abundances, which indicate the direction and magnitude of the species- and pathway-level shifts between LBD and control groups.

Analysis of microbial species prevalence data revealed additional differences in microbial composition between LBD and control groups. Six microbial species and two metabolic pathways were significantly more prevalent in LBD, while eight microbial species were more prevalent in controls (**Figure 3C**). When combined with the differential abundance results, several microbial species showed consistent patterns. Notably, Oscillospiraceae bacterium CLA-AA-H250 was not only more abundant in LBD but also present in a greater number of LBD individuals. Similarly, species such as *Eubacterium rectale*, GGB2653 SGB3574 (Firmicutes), and *Longicatena caecimuris* exhibited both higher relative abundance and prevalence in the control group, which indicates these taxa may serve as robust microbial signatures distinguishing LBD from controls.

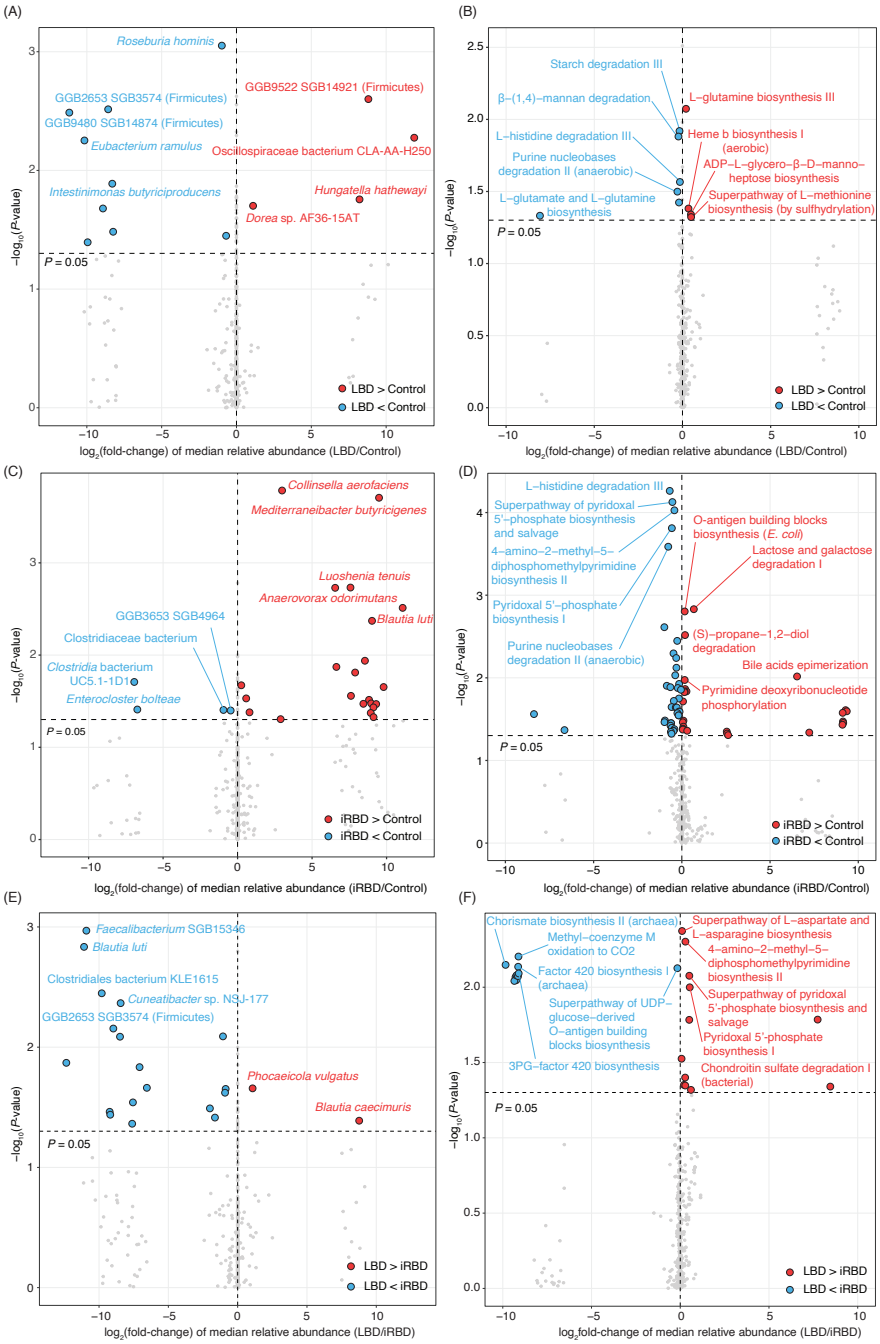

Figure 2. Volcano plots showing differentially abundant microbial species and metabolic pathways between LBD or iRBD and their cohabitant controls, as well as between LBD and iRBD.

$\log_2$(fold-change) was calculated based on the median relative abundance of each group. Statistical significance was defined at $P < 0.05$. Up to five microbial features are annotated for both positive and negative $\log_2$(fold-change) in each plot.

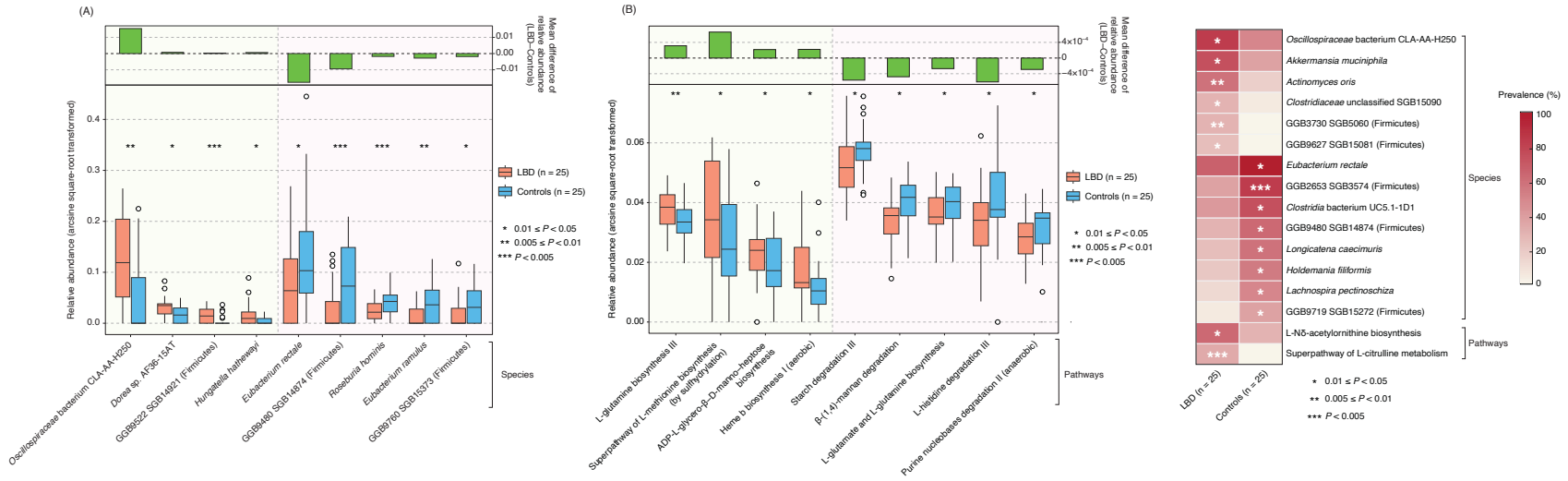

Figure 3. Differentially abundant and prevalent gut microbiome features between patients with LBD and their cohabitant controls.

(A–B) Boxplots show the top microbial species **(A)** and metabolic pathways **(B)**, up to five per panel if available, that were significantly different in relative abundance between LBD and control groups. P-values were obtained from mixed-effects linear regression models adjusting for age and sex, with household ID included as a random effect. Bar plots above each box represent the mean difference in relative abundance between LBD and control groups; positive values indicate features more abundant in LBD, while negative values indicate features more abundant in controls. **(C)** Heatmap shows microbial species and metabolic pathways that were significantly different in prevalence between groups. Color intensity reflects the proportion of individuals in each group carrying the corresponding feature. *P*-values were obtained from Fisher's exact test. *, $0.01 \le P < 0.05$; **, $0.005 \le P < 0.01$; ***, $P < 0.005$.

Differential abundance and prevalence between iRBD and cohabitant controls

After prevalence cut-off (described in the "Methods"), 573 microbial species and 439 metabolic pathways were kept for further differential analyses. A mixed-effects linear regression model was used to compare microbial species relative abundance between iRBD patients (n = 10) and their cohabitant controls (n = 10), adjusting for age and BMI and accounting for household ID as a random effect. This analysis revealed 22 microbial species that were significantly more abundant in the iRBD group, while four species showed higher abundance in controls (all $P < 0.05$; **Figure 2C**). Microbial species that were more abundant in the iRBD group included *Collinsella aerofaciens*, *Blautia luti*, *Mediterraneibacter butyricigenes*, *Luoshenia tenuis*, and *Anaerovorax odorimutans*; in contrast, the control group showed elevated levels of Clostridiaceae bacterium, GGB3653 SGB4964 (Firmicutes), Clostridia bacterium UC5.1-1D1, and *Enterocloster bolteae* (**Figure 4A**). Pathway analysis using the same approach identified 26 pathways that had significantly higher relative abundance in iRBD, as well as 39 pathways being more abundant in the control group (all $P < 0.05$; **Figure 2D**). Top 5 pathways enriched in iRBD included O-antigen building blocks biosynthesis (*E. coli*), lactose and galactose degradation I, pyrimidine deoxyribonucleotide phosphorylation, (S)-propane-1,2-diol degradation, and bile acids epimerization, while control group showed greater abundance of pathways such as 4-amino-2-methyl-5-diphosphomethylpyrimidine biosynthesis II, superpathway of pyridoxal 5'-phosphate biosynthesis and salvage, pyridoxal 5'-phosphate biosynthesis I, L-histidine degradation III, and purine nucleobases degradation II (anaerobic) (**Figure 4B**). Bar plots in the upper panels of **Figures 4A–B** demonstrate

the direction and magnitude of mean differences in relative abundances between the iRBD and controls.

In addition to differentially abundant microbial features, we identified three microbial species and one metabolic pathway that were significantly more prevalent in iRBD patients compared to their cohabitant controls (all $P < 0.05$; Fisher's exact test; **Figure 4C**). When integrating results from abundance and prevalence analyses, several features demonstrated consistent group-level differences. Specifically, *Luoshenia tenuis*, Clostridiaceae unclassified SGB15090, and the bile acids epimerization pathway were not only significantly more abundant in the iRBD group but also present in a greater proportion of iRBD individuals, which highlights these features as potential microbial markers associated with iRBD.

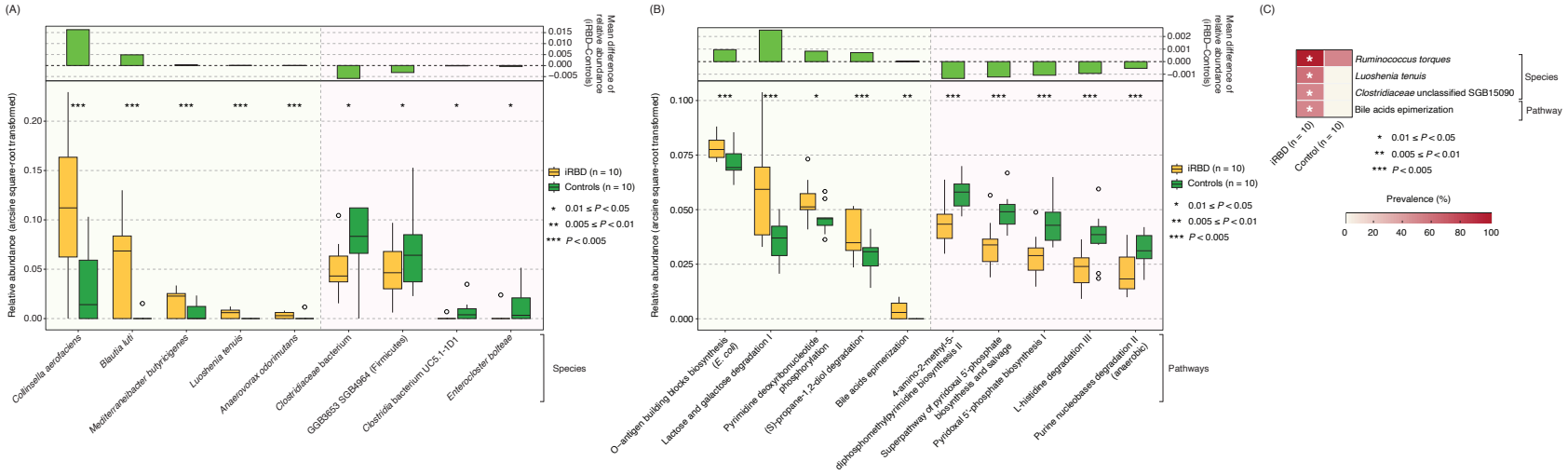

Figure 4. Differentially abundant and prevalent gut microbiome features between patients with iRBD and their cohabitant controls.

(A–B) Boxplots show the top microbial species **(A)** and metabolic pathways **(B)**, up to five per panel if available, that were significantly different in relative abundance between iRBD and control groups. *P*-values were obtained from mixed-effects linear regression models adjusting for age and sex, with household ID included as a random effect. Bar plots above each box represent the mean difference in relative abundance between iRBD and control groups; positive values indicate features more abundant in iRBD, while negative values indicate features more abundant in controls. **(C)** Heatmap shows microbial species and metabolic pathways that were significantly different in prevalence between groups. Color intensity reflects the proportion of individuals in each group carrying the corresponding feature. *P*-values were obtained from Fisher's exact test. *, $0.01 \le P < 0.05$; **, $0.005 \le P < 0.01$; ***, $P < 0.005$.

Differential abundance and prevalence between LBD and iRBD groups

To identify microbial features distinguishing LBD and iRBD patients, we performed differential abundance analysis on a filtered dataset of 512 species and 435 pathways using simple linear regression models adjusted for age and BMI. This revealed 20 species (2 enriched in LBD, 18 in iRBD) and 23 pathways (12 in LBD, 11 in iRBD) with significantly different relative abundance between groups (all $P < 0.05$, **Figures 2E–F**). For example, *Phocaeicola vulgatus* and *Blautia caecimuris* were more abundant in LBD, while *Blautia luti*, *Faecalibacterium* SGB15346, Clostridiales bacterium KLE1615, GGB2653 SGB3574 (Firmicutes), and *Cuneatibacter* sp. NSJ-177 were more abundant in iRBD (**Figure 5A**). At the pathway level, examples of pathways with higher abundance in LBD include superpathway of L-aspartate and L-asparagine biosynthesis, 4-amino-2-methyl-5-diphosphomethylpyrimidine biosynthesis II, superpathway of pyridoxal 5'-phosphate biosynthesis and salvage, Pyridoxal 5'-phosphate biosynthesis I, and Chondroitin sulfate degradation I (bacterial), whereas superpathway of UDP-glucose-derived O-antigen building blocks biosynthesis, chorismate biosynthesis II (archaea), Factor 420 biosynthesis I (archaea), Methyl-coenzyme M oxidation to CO_2, and 3PG-factor 420 biosynthesis were more abundant in iRBD (**Figure 5B**). The upper panels of **Figures 5A–B** summarize the direction and magnitude of these differences between LBD and iRBD using mean of relative abundances.

We also identified 26 species (5 in LBD, 21 in iRBD) and 12 pathways (2 in LBD, 10 in iRBD) with significantly different prevalence between the groups (all $P < 0.05$, Fisher's

exact test). The majority of these differentially prevalent features overlapped with those identified by abundance analysis.

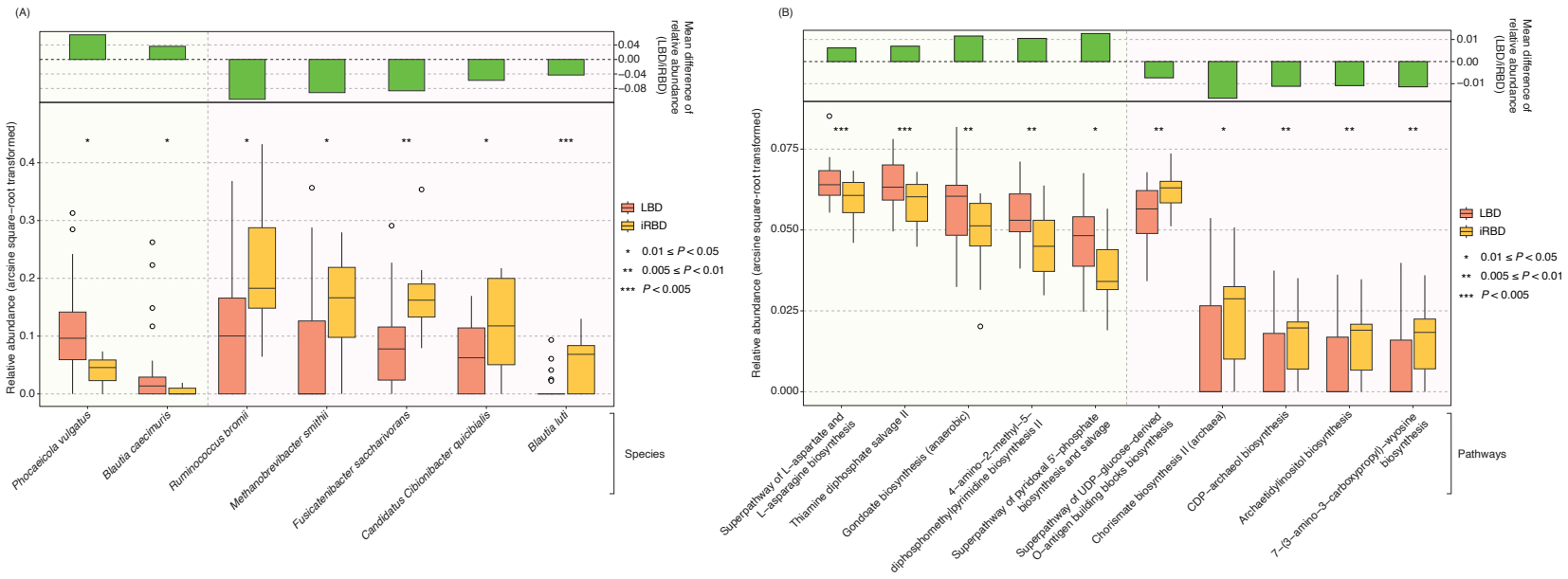

Figure 5. Differentially abundant gut microbiome features between patients with LBD and iRBD.

(A–B) Boxplots show the top microbial species **(A)** and metabolic pathways **(B)**, up to five per panel if available, that were significantly different in relative abundance between LBD and iRBD groups. *P*-values were obtained from a simple linear regression model adjusting for age and sex. Bar plots above each box represent the mean difference in relative abundance between LBD and iRBD groups; positive values indicate features more abundant in LBD, while negative values indicate features more abundant in iRBD. *, $0.01 \leq P < 0.05$; **, $0.005 \leq P < 0.01$; ***, $P < 0.005$.

Microbial features characterizing the disease continuum of Lewy body dementia

Several microbial features showed similar trends in both LBD and iRBD compared to their cohabitant controls, but statistical significance was observed only in LBD (**Figure 6D**). For example, Oscillospiraceae bacterium CLA-AA-H250, *Akkermansia muciniphila*, *Actinomyces oris*, GGB3730 SGB5060 (Firmicutes), and GGB9627 SGB15081 (Firmicutes) were more prevalent in both disease groups, but significant differences occurred only in LBD. On the contrary, Clostridia bacterium UC5.1-1D1, *Longicatena caecimuris*, and GGB9719 SGB15272 (Firmicutes) were more prevalent in cohabitant controls, again with significance limited to LBD. Similar patterns were seen for the superpathway of L-citrulline metabolism and L-Nδ-acetylornithine biosynthesis. These patterns suggest that microbial alterations may emerge in the early stage of disease (iRBD) but become statistically significant as the disease progresses to LBD.

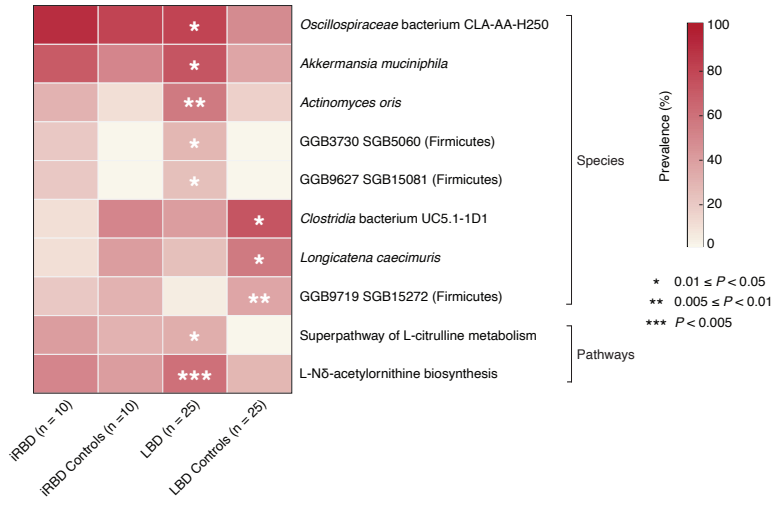

Figure 6. Progressive alterations in microbial species and pathways along the Lewy body dementia continuum.

Heatmap shows the prevalence of microbial species and metabolic pathways that are significantly different between LBD and controls. A similar trend is observed in iRBD compared to controls, although not statistically significant. Color intensity reflects the proportion of individuals in each group carrying the corresponding feature. P-values were obtained from Fisher's exact test. *, $0.01 \leq P < 0.05$; **, $0.005 \leq P < 0.01$; ***, $P < 0.005$.

Starch degradation III pathway in LBD and cohabitant controls

Among all pathways that were differentially abundant between LBD patients and cohabitant controls, starch degradation III was selected for further analysis because it showed the strongest statistical significance (mixed-effects linear regression model, $P = 0.012$) (**Figure 2B**).

Using HUMAnN3 functional profiling, we identified species-attributed contributions to starch degradation III in LBD patients and controls across 25 households (**Figure 7A**). These contributions showed clear inter-individual variability, with both the taxa contributing to the pathway and their proportional contributions varying across samples. Nevertheless, *Blautia obeum* and *Blautia wexlerae* consistently accounted for a high proportion of contributions across both groups. We then compared the total species-attributed contribution to starch degradation III between LBD patients and controls in each household. For each sample, this was calculated as the sum of species-stratified contributions identified by HUMAnN3 (**Figure 7A**). Using this definition, controls exhibited higher species-attributed contribution in 15 households (60%), whereas LBD patients showed higher contribution in 10 households (40%) (**Figure 7B**). At the species level, the relative abundance of the pathway contributed by *Eubacterium ramulus* was significantly higher in controls than LBD ($P = 0.012$) (**Figure 7C**).

Finally, mapping of gene families to enzymatic steps of starch degradation III indicated that there are more significant gene families being more abundant in controls for three of the four steps (**Figure 7D**). This pattern may suggest a potential reduction in microbial starch degradation capacity in LBD.

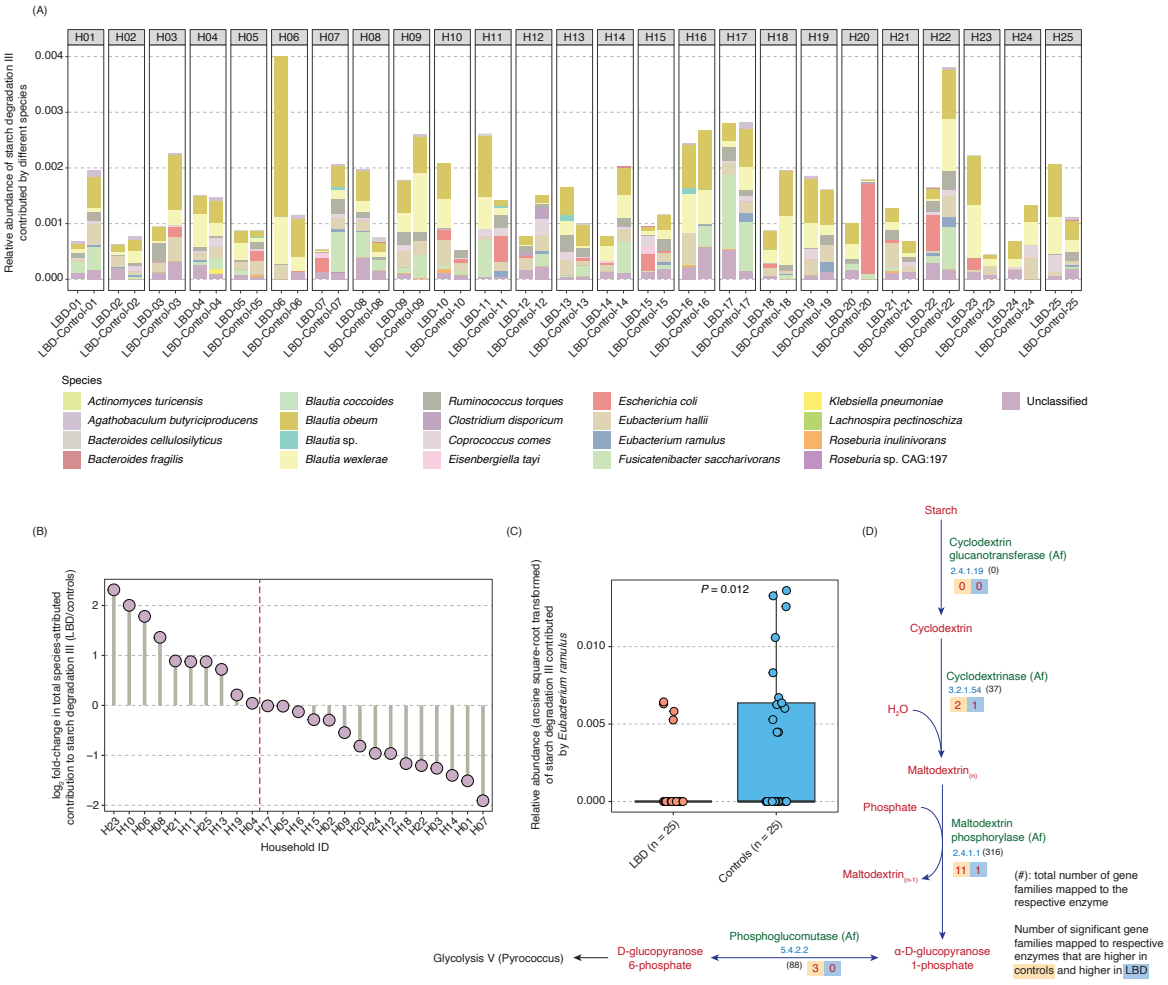

Figure 7. Comparison of the starch degradation III pathway between LBD and their cohabitant controls.

(A) Stacked bar plots for 25 households show the microbial species contributing to the starch degradation III pathway in matched LBD and control samples. Contributions from unmapped or unintegrated pathways were excluded. **(B)** For each household, the $\log_2$ fold-change in total microbial species' contributions to the starch degradation III pathway (LBD vs. controls) is shown. In ten households, LBD showed higher microbial contributions, while in fifteen households,

controls demonstrated greater microbial contributions. **(C)** Boxplot shows arcsine square-root transformed relative abundance of starch degradation III contributed by *Eubacterium ramulus*, which was significantly higher in controls compared with LBD patients. **(D)** Schematic diagram of the starch degradation III pathway highlights four key enzymes; each is annotated with the total number of gene families mapped (in parentheses). The numbers in the yellow and blue boxes represent the number of gene families mapped to the respective enzymes that are higher in controls and LBD, respectively.

Shared microbial features between LBD and iRBD compared to cohabitant controls

To gain insight into shared gut microbial alterations across disease stages, we identified features that were consistently different in both iRBD and LBD compared with controls. At the species level, Clostridiaceae unclassified SGB15090 was significantly more prevalent in both LBD and iRBD groups compared to their respective cohabitant controls (both $P < 0.05$; **Figures 3C** and **4C**). At the genus level, *Bacteroides* was significantly more abundant in both LBD and iRBD groups compared to their respective cohabitant controls (both $P < 0.05$; **Figure 8**). At the pathway level, the relative abundances of L-histidine degradation III, purine nucleobases degradation II (anaerobic), and L-glutamate and L-glutamine biosynthesis were consistently lower in both disease groups than in their cohabitant controls (all $P < 0.05$). These shared alterations may reflect common microbial or metabolic disruptions underlying both early and later stages of Lewy body dementia.

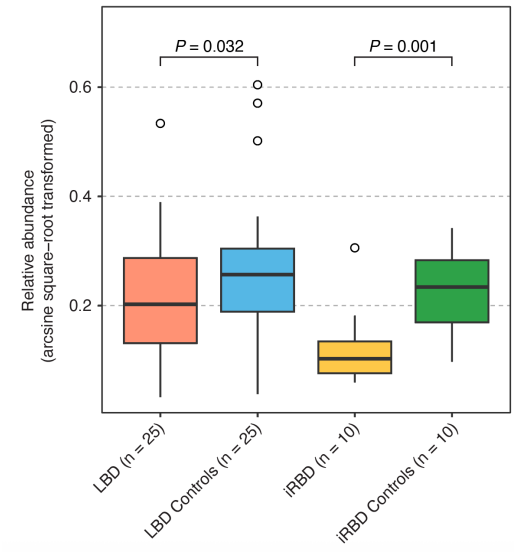

Figure 8. Boxplots showing the relative abundance of Bacteroides comparing between LBD or iRBD and their cohabitant controls.

P-values were obtained from mixed-effects linear regression models adjusting for age and sex, with household ID included as a random effect. Both LBD and iRBD patients had lower abundance of Bacteroides in their gut microbiome compared with their controls.

We further analyzed the L-histidine degradation III pathway to characterize its contributing microbial species and the associated gene families reflecting its functional potential. This pathway was significantly more abundant in cohabitant controls than in both LBD and iRBD groups ($P = 0.027$ and $P = 5.47\times10^{-5}$, respectively). Household-level stacked bar plots demonstrated obvious inter-individual variability in contributing species, with *Bacteroides uniformis* present as the most prevalent microbial contributor across all samples in LBD/iRBD and their cohabitant controls (**Figure 9A**). In most households, the total pathway abundance from all microbial contributors was higher in controls compared to cases (18/25 LBD households and 10/10 iRBD households), while 7 LBD households showed higher levels in LBD group. At the species-contributor level, the relative

abundance of the L-histidine degradation III pathway contributed by *Bacteroides eggerthii*, *Bacteroides dorei*, and *Bacteroides eggerthii* were higher in LBD (all $P < 0.05$; **Figures 9B–D**), whereas contribution from *Bacteroides thetaiotaomicron* was higher in iRBD ($P < 0.05$; **Figure 9E**). These findings indicates that lower abundance of L-histidine degradation III pathway in both LBD and iRBD groups might be associated with decreasing contributions from specific *Bacteroides* species.

The L-histidine degradation III pathway consists of multiple enzymes and intermediate compounds, as shown in **Figure 9F**. To investigate the functional potential of this pathway, gene families were mapped to each enzyme involved. It was observed that at almost every step, more gene families had higher abundance in controls compared with LBD and iRBD. In iRBD, several early steps already showed reduced gene family abundance, whereas in LBD, the reduction was especially pronounced in downstream folate metabolism (e.g., MTHFD1). These patterns suggest a loss of L-histidine degradation and related functional potential in both the prodromal (iRBD) and dementia (LBD) stages.

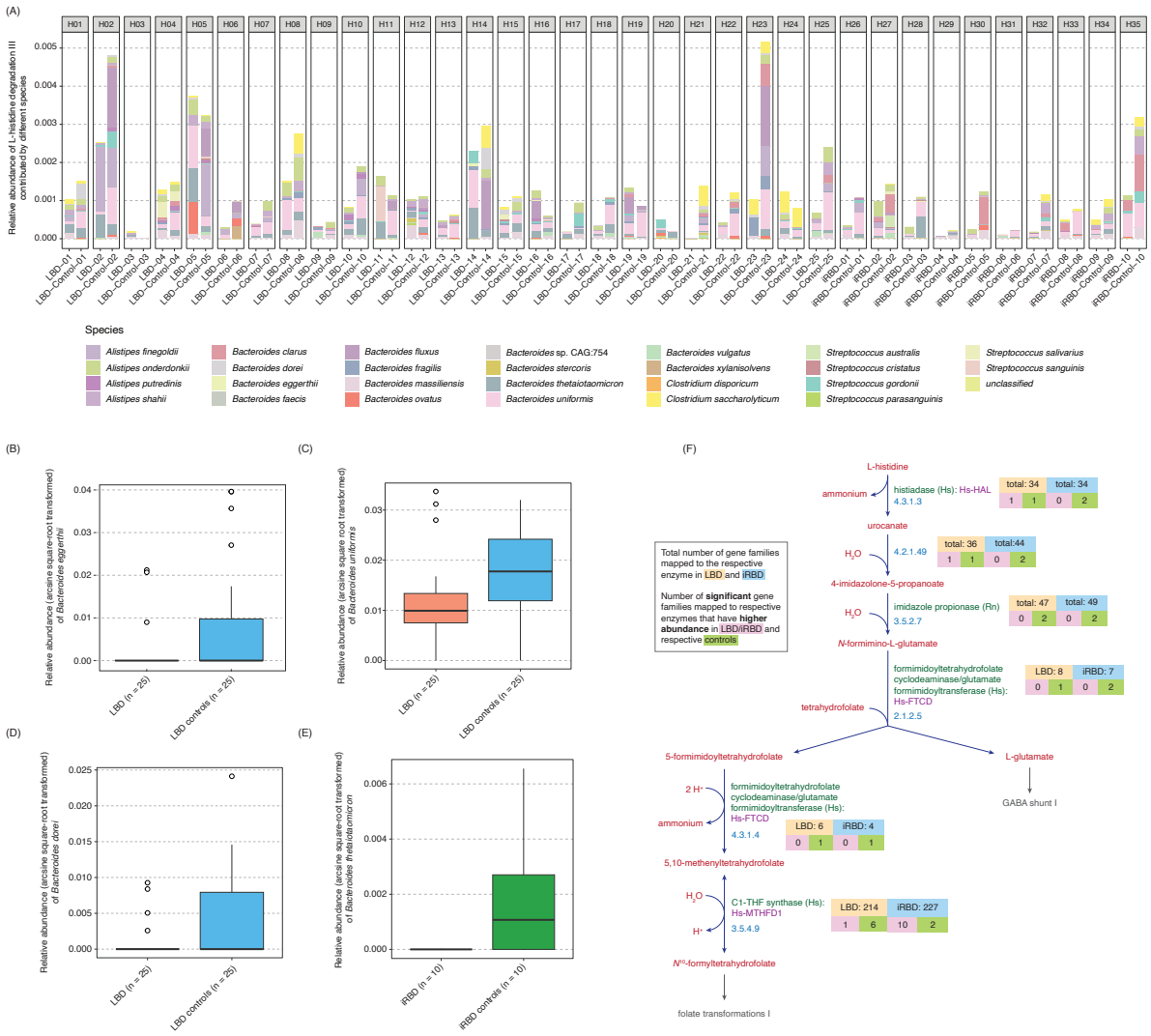

Figure 9. Comparison of the L-histidine degradation III pathway between LBD or iRBD and their cohabitant controls.

(A) Stacked bar plots for 35 households show the microbial species contributing to the L-histidine degradation III pathway in matched LBD or iRBD and control samples. Contributions from unmapped or unintegrated pathways were excluded. **(B–D)** Boxplots show arcsine square-root transformed relative abundances of the L-histidine degradation III pathway contributed by *Bacteroides eggerthii*, *Bacteroides dorei*, and *Bacteroides eggerthii*, which were significantly higher in controls than in LBD patients. **(E)** Similarly, *Bacteroides thetaiotaomicron* contributed to higher relative abundance of this pathway in controls than in iRBD patients. **(F)** Schematic diagram of the L-histidine degradation III pathway indicates multiple enzymes and intermediate compounds. In the figure, numbers in yellow boxes indicate the total number of gene families detected in LBD patients and their controls that were mapped to each enzyme, while numbers in blue boxes indicate those detected in iRBD patients and their controls. Numbers in pink boxes (bottom left) represent the number of significant gene families mapped to that enzyme with higher

abundance in the LBD or iRBD groups, whereas numbers in green boxes (bottom right) represent those with higher abundance in controls.

One of the final products of the L-histidine degradation III pathway is L-glutamate, which can enter the GABA synthesis pathway (GABA shunt) and be converted to γ-aminobutyric acid (GABA), an important neurotransmitter involved in the gut-brain axis. The key enzyme catalyzing this step is glutamate decarboxylase (EC 4.1.1.15). To investigate the potential of this enzyme in catalyzing the decarboxylation of L-glutamate to form GABA, we compared gene families mapped to this enzyme between LBD or iRBD and their cohabitant controls. In LBD, two differentially abundant gene families mapped to this enzyme showed higher abundance in controls, whereas in iRBD, one out of three differentially abundant gene families showed higher abundance in controls (**Figures 10A–7B**). This pattern suggests a gradual reduction in glutamate decarboxylase potential from the prodromal (iRBD) to the dementia (LBD) stage.

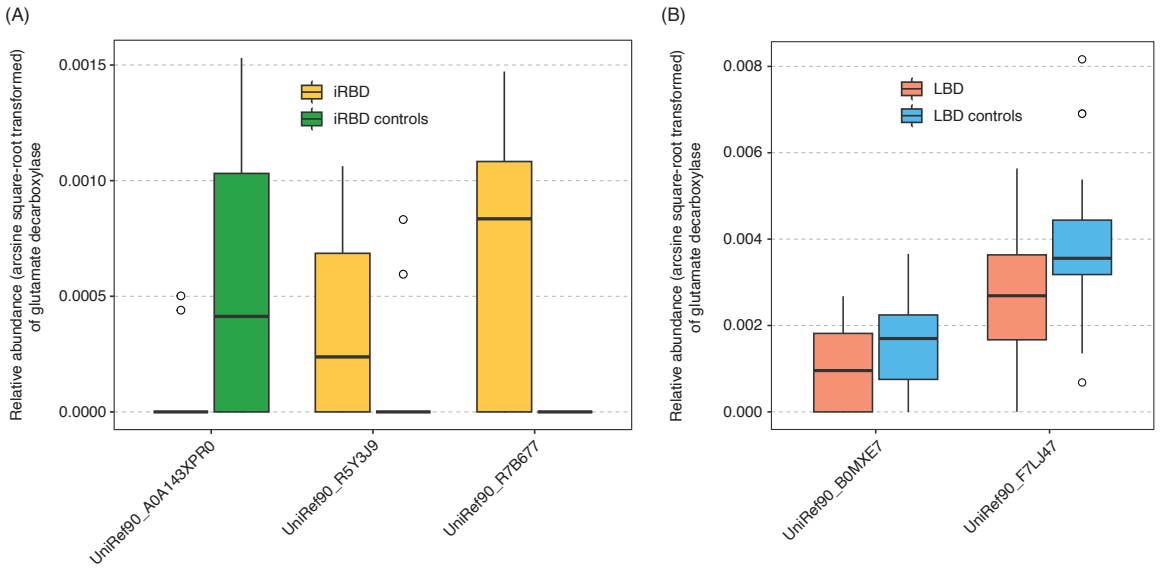

Figure 10. Boxplots of the relative abundances of gene families mapped to glutamate decarboxylase (EC 4.1.1.15).

(A) Three gene families were significantly different between iRBD and their cohabitant controls, among which one showed higher abundance in controls. **(B)** Two gene families were significantly different between LBD and their cohabitant controls, both showing higher abundance in controls.

Correlation between clinical features and microbial features

We calculated Spearman's correlation coefficients (ρ) and corresponding *P*-values between four clinical features (CDR-SB, MoCA, STMS, and MDS-UPDRS III) and the abundances of microbial species and metabolic pathways that were present in ≥ 40% of LBD samples and ≥ 80% of iRBD samples (**Figure 11A–B**). As more than 100 significant correlations were identified between microbial features and MDS-UPDRS III scores in LBD and iRBD patients, only key associations are presented here, and the full list of results is not shown. Among these clinical measures, CDR-SB, MoCA, and STMS evaluate dementia and cognitive impairment: higher CDR-SB scores indicate more severe dementia, whereas lower MoCA and STMS scores indicate greater cognitive

impairment. MDS-UPDRS III is used to evaluate the severity of motor symptoms in Parkinson's disease, with higher scores indicating worse impairment.

In LBD patients, *Christensenella hongkongensis* and Superpathway of L-alanine biosynthesis were negatively correlated with CDR-SB and positively correlated with both MoCA and STMS. In addition, Bifidobacterium shunt was positively correlated with MoCA and STMS, while Glycolysis II (from fructose 6-phosphate) and Homolactic fermentation were positively correlated with MoCA and negatively correlated with CDR-SB (**Figure 11A**), indicating that these features are associated with reduced severity of dementia and cognitive impairment. Superpathway of L-alanine biosynthesis, Bifidobacterium shunt, Glycolysis II (from fructose 6-phosphate), and Homolactic fermentation also showed negative correlations with MDS-UPDRS III, indicating associations with less severe motor symptoms. In contrast, L-arginine biosynthesis I (via L-ornithine) and L-arginine biosynthesis II (acetyl cycle) were positively correlated with MDS-UPDRS III, suggesting associations with more severe motor symptoms in LBD patients.

In iRBD patients, *Clostridium leptum* was positively correlated with MoCA scores and negatively correlated with CDR-SB. Additionally, *Coprococcus comes* and the (S)-propane-1,2-diol degradation pathway were positively correlated with both MoCA and STMS scores (**Figure 11B**). The myo-, chiro-, and scyllo-inositol degradation pathway was positively correlated with STMS but negatively correlated with MDS-UPDRS III scores. These findings suggest that these microbial features are associated with better cognitive performance and lower severity of cognitive and/or motor impairment in iRBD patients.

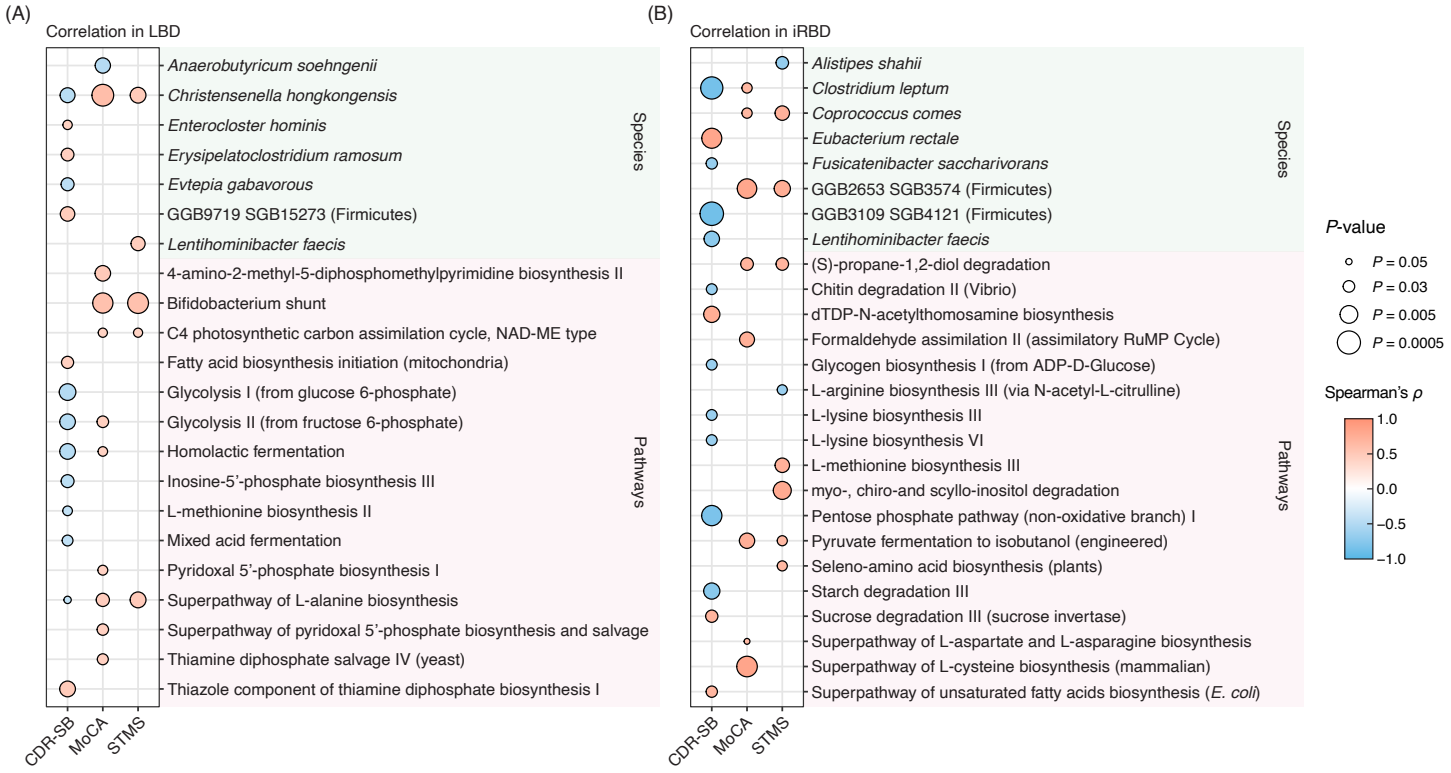

Figure 11. Correlations between clinical measures and gut microbial species and pathways in (A) LBD and (B) iRBD.

Spearman correlation coefficients and corresponding *P*-values were calculated for each clinical measure. Each bubble represents a significant correlation ($P < 0.05$) with a Spearman's $|\rho| > 0.35$. Positive correlations are shown in red, and negative correlations in blue. Only microbial species and pathways meeting both significance and effect size thresholds are represented. Notably, several microbial features were associated with cognitive scores (CDR-SB, MoCA, STMS). No microbial features showed a significant correlation with MMSE in iRBD. Bubble size reflects the strength of the P-value, with smaller values shown as larger bubbles. CDR-SB, Clinical Dementia Rating Sum of Boxes; MoCA, Montreal Cognitive Assessment; STMS, Short Test of Mental Status.

Discussion

In this study, we compared the gut microbiome taxonomic and metabolic functional profiles between prodromal (iRBD) and late (LBD) stages of Lewy body dementia and their cohabitant controls. Our main aim was to identify stage-specific and shared alterations in microbial features, including both taxonomic shifts and functional differences shown by enriched metabolic pathways and gene families potentially relevant to LBD-related pathophysiology.

Overall, α-diversity indices at the species level, specifically Shannon index and richness, showed no significant differences between LBD/iRBD patients and controls. Similarly, β-diversity analyses using PERMANOVA demonstrated no significant differences in the overall gut microbial community structure between patients and controls. These findings suggest that, at a community-wide level, gut microbial diversity and composition are not significantly perturbed in LBD or iRBD. The lack of significant separation is likely influenced by the use of household-matched controls, who share similar environmental exposures and dietary habits, and have close contact with the patients. Previous studies have demonstrated that cohabiting individuals often harbor more similar gut microbiota compared to unrelated individuals, indicating the strong influence of shared environment and lifestyle[61,67].

Although no overall differences in the gut microbiome communities were observed at the community level between patients and controls, finer-scale taxonomic alterations were still detected between groups. We first analyzed gut microbiome to examine whether any gut microbes are unique to LBD and iRBD. Analysis of microbial taxa at both the

genus and species levels revealed several significant differences between LBD or iRBD patients and controls, indicating both

Specifically, we observed a higher abundance of *Hungatella hathewayi* in LBD and *Collinsella aerofaciens* in iRBD. *H. hathewayi* has been reported to be more abundant in multiple conditions, including multiple sclerosis[68], colorectal cancer[69], and eczema[70]. Rawat *et al.* demonstrated that *H. hathewayi* can degrade glycosaminoglycans (GAGs) [71], which are structural components of the intestinal extracellular matrix and glycocalyx that support epithelial barrier integrity[72]. Experimental studies have shown that excessive depletion of GAG-rich layers in other epithelia and in the vasculature markedly increases tissue permeability, suggesting that over-degradation of GAGs may weaken barrier function[73,74]. In this context, the higher abundance of *H. hathewayi* observed in LBD may contribute to impaired intestinal barrier integrity and systemic inflammation, thereby potentially increasing CNS vulnerability to pathological processes. We also observed higher abundance of *C. aerofaciens* in iRBD compared with controls. This species and its genus have previously been reported to be overrepresented in RBD[46], early PD[46], and DLB[47], as well as in elderly individuals with severe cognitive impairment[75]. Beyond neurodegeneration, *Collinsella* was found to be more abundant in rheumatoid arthritis, where it has been shown in mouse models to reduce the tight junction protein ZO-1 and to increase gut permeability[76]. The same study further suggested that *Collinsella* stimulates IL-17A production in intestinal epithelial cells, and linked it to pro-inflammatory responses with a loss of gut epithelial integrity[76]. Therefore, our findings might indicate both *H. hathewayi* and *C. aerofaciens* may contribute to gut barrier dysfunction and

systemic inflammation during the course of α-synucleinopathies. However, further experimental work and mechanistic validation are needed to determine how they influence disease progression in LBD.

Additional taxa also showed decreased abundance in LBD and iRBD. For example, *Roseburia hominis*, *Eubacterium ramulus*, and *Intestinimonas butyriciproducens* were decreased in LBD, while an unclassified Clostridiaceae bacterium was reduced in iRBD compared with their cohabitant controls. In addition, the genus *Bacteroides* was consistently reduced in both groups. These taxa are well recognized for their contributions to dietary fiber fermentation and short-chain fatty acid (SCFA) production[77-80]. *R. hominis* and *I. butyriciproducens* are established butyrate and propionate producers[77,79], while *E. ramulus* degrades flavonoids and supports butyrate formation through cross-feeding[81]. *Bacteroides* species mainly produce acetate and propionate, which can act both as signaling molecules and as substrates for butyrate producers[82-84]. Members of the Clostridiaceae family are also obligate anaerobes that ferment carbohydrates to generate SCFAs, particularly acetate and butyrate. Therefore, the depletion of these beneficial commensals suggests a shared signature of reduced SCFA production capacity in both prodromal (iRBD) and dementia (LBD) stages, which may compromise gut barrier integrity and disrupt gut-brain axis signaling throughout the disease progression.

In addition to microbial compositional differences, the metagenomic functional profiling can further provide insights into how the gut microbiome may influence host physiology in context of LBD through microbial metabolism. The gut microbiome plays a key role in the gut-brain axis. One of the main ways the microbiome participates in this

system is through the production of metabolites that can affect immune, endocrine, and neuronal signaling pathways[52,85-87]. Our findings suggest that metabolic alterations in iRBD and/or LBD may reflect a shift in microbial functions that modulate gut-brain communication.

We first focused on microbial metabolic pathways involved in the production of SCFAs. In our study, the starch degradation III pathway was significantly less abundant in LBD than in controls (P = 0.012), with multiple gene families encoding maltodextrin phosphorylase and phosphoglucomutase reduced in LBD. This pathway represents a bacterial mechanism that converts dietary starch into glycolytic intermediates for energy extraction[88,89]. The final product of this pathway, D-glucopyranose-6-phosphate, feeds into glycolysis, where it is metabolized to pyruvate and further converted to acetate[88,90]. Acetate can not only serve as a co-substrate for microbial butyrate synthesis, but can also reach the central nervous system, where it acts as a preferred energy source for astrocytes and supports the maintenance of glutamate and GABA levels, which are the main excitatory and inhibitory neurotransmitters in the brain[91,92]. Once inside the brain, acetate is converted to acetyl-CoA, a key substrate for histone acetylation[93,94]. Mews *et al.* demonstrated that microbial-derived acetate contributes to brain histone acetylation and modulates memory-related gene expression[94]. Therefore, the reduced abundance of the starch-degrading pathway in LBD can suggest decreased acetate production, which may compromise gut barrier integrity, alter epigenetic regulation and neural plasticity, and contribute to an imbalance of excitatory and inhibitory neurotransmission along the gut-brain axis.

Another key mechanism involves microbial modulation of neurotransmitter availability. In our study, the L-histidine degradation III pathway showed lower abundance in both LBD and iRBD compared with their respective controls. Furthermore, multiple gene families involved in different steps of this pathway were also reduced in LBD and iRBD. The L-histidine degradation III pathway is a microbial route for histidine catabolism in the gut, in which histidine is converted to L-glutamate and other final products. L-glutamate can enter the GABA shunt pathway, where it is converted to GABA by the enzyme glutamate decarboxylase. Our results demonstrated among all gene families that are mapped to glutamate decarboxylase, in LBD, two differentially abundant gene families showed higher abundance in controls, whereas in iRBD, one out of three differentially abundant gene families showed higher abundance in controls. These results indicate that the potential capability of converting from L-glutamate to GABA gradually decreased from iRBD to LBD. GABA and glutamate are the principal inhibitory and excitatory neurotransmitters in the brain, respectively, and alterations in their signaling have been implicated in the pathophysiology of neurodegenerative diseases[95,96]. Increasing evidence suggests that gut-derived GABA can influence its levels in the bloodstream and the brain, which indicates the gut microbiome's potential role on regulating GABA-related neural signaling and neurological health[52,97]. Previous studies have shown that reduced potential of gut-derived GABA being observed across multiple neurodegenerative conditions. Marzouk *et al*. found higher abundance of GABA-consuming species in PD samples compared with health controls[98]. Wallen *et al*. utilized shotgun metagenomic sequencing and observed an increase in glutamate and GABA degradation but a

decrease in glutamate/glutamine synthesis gene families and pathways in PD patients, which indicates a systemic imbalance in GABA homeostasis driven by gut microbiota[99]. Recent studies have investigated the potential of probiotics and prebiotics for targeting microbial GABA metabolism. Treatment with the probiotic *Pediococcus pentosaceus* or the prebiotic polymannuronic acid improved gut microbial balance and restored GABA levels in the brains of MPTP-induced mice, which lead to reduced motor impairment and neuronal loss[100]. In addition, a recent randomized controlled trial in PD patients showed that co-administration of probiotics with conventional therapy increased microbial species involved in GABA synthesis and decreased those associated with GABA degradation, compared with conventional therapy alone[101]. Therefore, combined with the results from our study, we hypothesize that reduced microbial histidine degradation in both LBD and iRBD may lower glutamate production in the gut and reduce the flux feeding into the GABA shunt. We also observed reduced microbial capacity to convert glutamate into GABA, indicating less GABA may be produced. Because GABA is the main inhibitory neurotransmitter in the central nervous system, changes in microbial glutamate and GABA metabolism may disturb the excitatory-inhibitory balance along the gut-brain axis. This imbalance may weaken neuroprotection and contribute to the pathogenesis of LBD.

Some microbial metabolic pathways generate products that can activate host immune signaling and contribute to systemic and neuroinflammation. In fact, we observed pathways associated with pro-inflammatory bacterial components were increased in both disease groups. Specifically, we found increased abundance of the ADP-L-glycero-β-D-manno-heptose biosynthesis pathway in LBD and the O-antigen building blocks

biosynthesis pathway in iRBD. The final products of both pathways are essential components for lipopolysaccharide (LPS) assembly. ADP-L-glycero-β-D-manno-heptose serves as a precursor for the inner core[102,103], and O-antigen building blocks form the outer polysaccharide part of LPS[103,104]. Using bacterial morphological information from BacDive[140], we examined and compared the total relative abundance of all Gram-negative bacterial species. However, no significant differences were observed between individuals with LBD or iRBD and their cohabitant controls. LPS is a structural component of Gram-negative bacterial cell walls and a major endotoxin[104,105], and based on previous studies, increased levels of LPS could have several important consequences relevant to α-synucleinopathies. First, LPS is known to compromise gut epithelial barrier integrity and promote intestinal permeability[106-108]. This allows exposure of the enteric nervous system to luminal antigens such as bacterial molecules and other substances[109]. More importantly, LPS may directly contribute to the initiation of α-synuclein aggregation in the gut. Several in vitro studies have shown that LPS accelerates α-synuclein fibrillization by promoting the formation of nucleating intermediates[110,111]. In addition, translocation of LPS into the circulation can activate innate immune pathways via toll-like receptors, stimulating production of pro-inflammatory cytokines (e.g., IL-1β, TNF-α, IL-6) and reactive oxygen substances[112-114]. These immune responses promote microglial activation and have been linked to neuronal loss in the substantia nigra and motor deficits in animal models[115-117]. Overall, our results suggest that the increased abundance of LPS-producing-related pathways in both iRBD and LBD may indicate enhanced microbial

potential for endotoxin production, which potentially contributes to increased intestinal permeability and facilitates α-synuclein aggregation within the gut.

Finally, we examined associations between gut microbiome features and clinical measures of cognition and motor performance in both LBD and iRBD patients. No shared correlation features were found between the two groups, suggesting that each disease stage has distinct microbiome-clinical relationships. This supports the idea that iRBD and LBD represent separate phases along the same disease continuum, each with stage-specific microbial signatures that may reflect different mechanisms of progression.

More specifically, *C. hongkongensis* was positively associated with reduced cognitive impairment and dementia in LBD patients, while *Clostridium leptum* and *Coprococcus comes* showed similar associations in iRBD patients. Although the metabolic capacity of *C. hongkongensis* has not been well studied, its placement within the *Christensenellaceae* family suggests functional similarity to other *Christensenella* species. *Christensenella minuta*, which shares 96.5% sequence identity with *C. hongkongensis*[118], has been reported to support intestinal barrier integrity[119], regulate inflammation[120], and produce short-chain fatty acids such as butyrate[121]. The observed negative correlation of *C. hongkongensis* with dementia and cognitive impairment severity in LBD patients may reflect potential metabolic benefits of more species within Christensenellaceae family. Similarly, *Clostridium leptum* and *Coprococcus comes* are established butyrate producers in the human gut[122], which is consistent with their positive association with reduced dementia severity in iRBD patients.

Several microbial metabolic pathways were associated with clinical measures in LBD. The Superpathway of L-alanine biosynthesis and the Bifidobacterium shunt both showed negative correlations with cognitive and motor impairment, suggesting that loss of those key microbial metabolic functions may contribute to disease severity. Alanine metabolism is closely connected to glutamate and glutamine cycling, which support neurotransmission and neuronal energy balance[123,124]. Experimental studies have shown that alanine helps transfer carbon and nitrogen between neurons and glial cells to support brain energy metabolism and excitatory neurotransmitter production[125,126]. Reduced microbial potential for Superpathway of L-alanine biosynthesis may therefore impair these metabolic processes and make neurons more vulnerable and less resilience in α-synuclein-related pathology.

The Bifidobacterium shunt pathway is a carbohydrate metabolism pathway found mainly in *Bifidobacterium*, which converts various sugars into acetate and lactate[127,128]. Acetate and lactate can serve as substrates for other gut bacteria to produce butyrate, which help protect the intestinal barrier and support overall colon health[129-131]. Because of these effects, the Bifidobacterium shunt pathway is often linked to gut health, anti-inflammatory functions, and neuroprotective potential through the gut-brain axis[127]. In our study, the negative correlation between the abundance of the Bifidobacterium shunt pathway and cognitive and motor impairment in LBD suggests that its beneficial metabolic functions may play a protective role against disease progression.

In iRBD patients, cognitive (STMS) and motor (MDS-UPDRS III) impairment were positively associated with reduced abundance of the myo-, chiro-, and scyllo-inositol

degradation pathway, whereas higher abundance of the (S)-propane-1,2-diol degradation pathway was correlated with better cognitive performance (MoCA and STMS). Elevated myo-inositol detected in cerebrospinal fluid or by brain imaging is widely regarded as a marker of gliosis and neuroinflammation, and several studies have proposed that myo-inositol accumulation serves as an early biomarker of Alzheimer's disease progression[132,133]. Given that elevated myo-inositol is linked to neuroinflammation, microbial degradation of inositols in the gut may help lower systemic levels of these metabolites and potentially influence brain inflammation through the gut-brain axis[134,135]. In our study, greater abundance of the myo-, chiro-, and scyllo-inositol degradation pathway was associated with better cognitive and motor performance in iRBD, the prodromal stage of LBD. It is possible that higher abundance of this pathway reflects a potential microbial capacity to lower systemic inositol levels, which could be linked to reduced neuroinflammatory signaling. The finding that higher abundance of the (S)-propane-1,2-diol degradation pathway was correlated with better cognitive performance (MoCA and STMS) suggests a potential beneficial role of this microbial metabolic function. (S)-propane-1,2-diol is an intermediate generated from the fermentation of fucose and rhamnose, which are derived from dietary sources and mucin in the gut[136,137]. Its degradation is carried out by certain commensal bacteria and leads to the production of SCFAs such as propionate and butyrate[138,139]. SCFAs are known to support gut barrier integrity, regulate immune responses, and modulate neuroinflammation through the gut-brain axis. Thus, greater microbial potential for (S)-propane-1,2-diol degradation could reflect a community structure enriched in beneficial fermentative activity, with downstream

SCFA production contributing to healthier systemic and neuroimmune signaling. Overall, all the findings above suggest that alterations in gut microbiome composition and function are associated with cognitive and motor severity in both LBD and iRBD patients.

Limitations

Several limitations of our study should be acknowledged when interpreting these findings. First, we could not adjust for sex when identifying differentially abundant microbial features due to the strong collinearity between sex and disease status in our cohort. Because patients and controls were household-matched, each pair necessarily differed by sex. Adjusting for sex in mixed-effects linear models would not distinguish the effects of sex from those of disease status, potentially masking true disease-related signals. Nevertheless, using household-matched controls in this study remains a strength because it helps reduce variation caused by different environment and lifestyle factors.

Second, although we recruited cohabitant controls to reduce environmental and lifestyle variability, we did not record the degree to which dietary habits were shared. As a result, dietary influences may not have been fully controlled by household matching. Even so, using of cohabitant controls still provides a valuable design for controlling many unmeasured environmental factors that are difficult to capture in unrelated control studies.

Third, the relatively small sample size, especially for the iRBD group and their matched controls (n = 10), can reduce statistical power and increases the likelihood that true effects were underestimated or not detected. Recruiting well-characterized iRBD and LBD patients, along with their cohabitant controls, is somehow challenging due to the rarity of these conditions, strict diagnostic criteria, and the need for matched household participation. Despite these difficulties, the consistent patterns observed across related microbial taxa and pathways suggest that the identified features are biologically meaningful and can be further validated in larger cohorts.

Fourth, we did not apply multiple hypothesis testing correction because no results remained significant after adjustment. This raises the possibility that some reported associations may represent false positives. However, these findings can still serve as useful hypotheses for future studies with greater statistical power.

Finally, our findings demonstrate correlations between microbial features and disease stage or progression, but no causal relationships can be inferred in the absence of experimental validation. However, these results still highlight the important links between the microbiome and host pathology in LBD, suggesting that gut microbial alterations may influence processes such as inflammation, barrier function, or α-synuclein aggregation. These associations could be further investigated through longitudinal studies and experimental models to better understand their potential mechanistic roles in disease progression.

Despite these limitations, our study provides one of the first comparative taxonomic and functional profiles of the gut microbiome using shotgun metagenomic sequencing across the prodromal (iRBD) and dementia (LBD) stages, providing important insights into potential microbial features linked to disease progression.

Conclusions

This study provides a comprehensive view of gut microbiome alterations across the LBD disease continuum from the prodromal stage (iRBD) to the late stage (LBD). Our findings suggest an increase in microbes that may weaken gut barrier function and increase gut permeability, along with a loss of beneficial microbes that support gut integrity and neuroprotective signaling. At the functional level, reduced microbial capacity for producing SCFAs and GABA, together with increased abundance of pathways related to lipopolysaccharide biosynthesis, indicates enhanced pro-inflammatory microbial activity and disrupted gut-brain communication that may contribute to early α-synuclein pathology. Moreover, several microbial species and metabolic pathways were associated with better cognitive and motor performance, suggesting potential protective roles of specific gut microbes.

Overall, our results highlight the importance of the gut microbiome in the pathophysiology of Lewy body dementia. Microbial dysbiosis and functional decline appear to be common features across both iRBD and LBD and may play an important role in driving neuroinflammatory and neurodegenerative processes. We expect that our work will serve as one cornerstone for understanding the microbiome's contribution to disease mechanisms along the Lewy body disease spectrum and for guiding future research into microbiome-based diagnostics and therapeutic interventions.

References

1. Kane JPM, Surendranathan A, Bentley A, et al. Clinical prevalence of Lewy body dementia. *Alzheimers Res Ther*. 2018;10(1):19. doi:10.1186/s13195-018-0350-6.

2. Vann Jones SA, O'Brien JT. The prevalence and incidence of dementia with Lewy bodies: a systematic review of population and clinical studies. *Psychol Med*. 2014;44(4):673-83. doi:10.1017/s0033291713000494.

3. Kalra S, Bergeron C, Lang AE. Lewy body disease and dementia. A review. *Arch Intern Med*. 1996;156(5):487-93. doi:10.1001/archinte.1996.00440050031004.

4. Braak H, Tredici KD, Rüb U, et al. Staging of brain pathology related to sporadic Parkinson's disease. *Neurobiology of Aging*. 2003;24(2):197-211. doi:10.1016/S0197-4580(02)00065-9.

5. Wong YC, Krainc D. α-synuclein toxicity in neurodegeneration: mechanism and therapeutic strategies. *Nature Medicine*. 2017;23(2):1-13. doi:10.1038/nm.4269.

6. Stefanis L. α-Synuclein in Parkinson's disease. *Cold Spring Harb Perspect Med*. 2012;2(2):a009399. doi:10.1101/cshperspect.a009399.

7. Schulz-Schaeffer WJ. The synaptic pathology of α-synuclein aggregation in dementia with Lewy bodies, Parkinson's disease and Parkinson's disease dementia. *Acta Neuropathologica*. 2010;120(2):131-143. doi:10.1007/s00401-010-0711-0.

8. McKeith IG, Boeve BF, Dickson DW, et al. Diagnosis and management of dementia with Lewy bodies: Fourth consensus report of the DLB Consortium. *Neurology*. 2017;89(1):88-100. doi:10.1212/wnl.0000000000004058.

9. Walker Z, Possin KL, Boeve BF, et al. Lewy body dementias. *The Lancet*. 2015;386(10004):1683-1697. doi:10.1016/S0140-6736(15)00462-6.

10. Donaghy PC, McKeith IG. The clinical characteristics of dementia with Lewy bodies and a consideration of prodromal diagnosis. *Alzheimer's Research & Therapy*. 2014;6(4):46. doi:10.1186/alzrt274.

11. Sabbagh MN, Taylor A, Galasko D, et al. Listening session with the US Food and Drug Administration, Lewy Body Dementia Association, and an expert panel. *Alzheimer's & Dementia: Translational Research & Clinical Interventions*. 2023;9(1):e12375. doi:10.1002/trc2.12375.

12. Hu MT. REM sleep behavior disorder (RBD). *Neurobiology of Disease*. 2020;143:104996. doi:10.1016/j.nbd.2020.104996.

13. Sobreira-Neto MA, Stelzer FG, Gitaí LLG, et al. REM sleep behavior disorder: update on diagnosis and management. *Arq Neuropsiquiatr*. 2023;81(12):1179-1194. doi:10.1055/s-0043-1777111.

14. Stefani A, Antelmi E, Arnaldi D, et al. From mechanisms to future therapy: a synopsis of isolated REM sleep behavior disorder as early synuclein-related disease. *Mol Neurodegener*. 2025;20(1):19. doi:10.1186/s13024-025-00809-0.

15. Lu J, Sherman D, Devor M, Saper CB. A putative flip-flop switch for control of REM sleep. *Nature*. 2006;441(7093):589-594. doi:10.1038/nature04767.

16. Peever J, Luppi PH, Montplaisir J. Breakdown in REM sleep circuitry underlies REM sleep behavior disorder. *Trends in Neurosciences*. 2014;37(5):279-288. doi:10.1016/j.tins.2014.02.009.

17. Boeve BF, Silber MH, Ferman TJ, et al. Clinicopathologic correlations in 172 cases of rapid eye movement sleep behavior disorder with or without a coexisting neurologic disorder. *Sleep Medicine*. 2013;14(8):754-762. doi:10.1016/j.sleep.2012.10.015.

18. Boeve BF, Dickson DW, Olson EJ, et al. Insights into REM sleep behavior disorder pathophysiology in brainstem-predominant Lewy body disease. *Sleep Medicine*. 2007;8(1):60-64. doi:10.1016/j.sleep.2006.08.017.

19. Townsend LTJ, Anderson KN, Boeve BF, et al. Sleep disorders in Lewy body dementia: Mechanisms, clinical relevance, and unanswered questions. *Alzheimer's & Dementia*. 2023;19(11):5264-5283. doi:10.1002/alz.13350.

20. Iranzo A, Tolosa E, Gelpi E, et al. Neurodegenerative disease status and post-mortem pathology in idiopathic rapid-eye-movement sleep behaviour disorder: an observational cohort study. *Lancet Neurol*. 2013;12(5):443-53. doi:10.1016/s1474-4422(13)70056-5.

21. Galbiati A, Verga L, Giora E, et al. The risk of neurodegeneration in REM sleep behavior disorder: A systematic review and meta-analysis of longitudinal studies. *Sleep Medicine Reviews*. 2019;43:37-46. doi:10.1016/j.smrv.2018.09.008.

22. Iranzo A, Santamaria J, Tolosa E. The clinical and pathophysiological relevance of REM sleep behavior disorder in neurodegenerative diseases. *Sleep Medicine Reviews*. 2009;13(6):385-401. doi:10.1016/j.smrv.2008.11.003.

23. Olson EJ, Boeve BF, Silber MH. Rapid eye movement sleep behaviour disorder: demographic, clinical and laboratory findings in 93 cases. *Brain*. 2000;123(2):331-339. doi:10.1093/brain/123.2.331.

24. Boeve BF, Silber MH, Ferman TJ, et al. REM sleep behavior disorder and degenerative dementia. *Neurology*. 1998;51(2):363-370. doi:10.1212/WNL.51.2.363.

25. Ferman TJ, Boeve BF, Smith GE, et al. REM sleep behavior disorder and dementia. *Neurology*. 1999;52(5):951-951. doi:10.1212/WNL.52.5.951.

26. Boeve BF, Silber MH, Parisi JE, et al. Synucleinopathy pathology and REM sleep behavior disorder plus dementia or parkinsonism. *Neurology*. 2003;61(1):40-45. doi:10.1212/01.WNL.0000073619.94467.B0.

27. Högl B, Stefani A, Videnovic A. Idiopathic REM sleep behaviour disorder and neurodegeneration — an update. *Nature Reviews Neurology*. 2018;14(1):40-55. doi:10.1038/nrneurol.2017.157.

28. Postuma RB, Berg D. Prodromal Parkinson's Disease: The Decade Past, the Decade to Come. *Movement Disorders*. 2019;34(5):665-675. doi:10.1002/mds.27670.

29. McKeith IG, Dickson DW, Lowe J, et al. Diagnosis and management of dementia with Lewy bodies. *Neurology*. 2005;65(12):1863-1872. doi:10.1212/01.wnl.0000187889.17253.b1.

30. Mayer EA. Gut feelings: the emerging biology of gut–brain communication. *Nature Reviews Neuroscience*. 2011;12(8):453-466. doi:10.1038/nrn3071.

31. Mayer EA, Tillisch K, Gupta A. Gut-brain axis and the microbiota. *J Clin Invest*. Mar 2 2015;125(3):926-38. doi:10.1172/jci76304.

32. Cryan JF, O'Riordan KJ, Cowan CSM, et al. The Microbiota-Gut-Brain Axis. *Physiol Rev*. 2019;99(4):1877-2013. doi:10.1152/physrev.00018.2018.

33. Loh JS, Mak WQ, Tan LKS, et al. Microbiota-gut-brain axis and its therapeutic applications in neurodegenerative diseases. *Signal Transduction and Targeted Therapy*. 2024;9(1):37. doi:10.1038/s41392-024-01743-1.

34. Savulescu-Fiedler I, Benea SN, Căruntu C, et al. Rewiring the Brain Through the Gut: Insights into Microbiota-Nervous System Interactions. *Curr Issues Mol Biol*. 2025;47(7). doi:10.3390/cimb47070489.

35. Sampson Timothy R, Mazmanian Sarkis K. Control of Brain Development, Function, and Behavior by the Microbiome. *Cell Host & Microbe*. 2015;17(5):565-576. doi:10.1016/j.chom.2015.04.011.

36. Vogt NM, Kerby RL, Dill-McFarland KA, et al. Gut microbiome alterations in Alzheimer's disease. *Scientific Reports*. 2017;7(1):13537. doi:10.1038/s41598-017-13601-y.

37. Jiang C, Li G, Huang P, et al. The Gut Microbiota and Alzheimer's Disease. *Journal of Alzheimer's Disease*. 2017;58(1):1-15. doi:10.3233/jad-161141.

38. Strati F, Cavalieri D, Albanese D, et al. New evidences on the altered gut microbiota in autism spectrum disorders. *Microbiome*. 2017;5(1):24. doi:10.1186/s40168-017-0242-1.

39. Vuong HE, Hsiao EY. Emerging Roles for the Gut Microbiome in Autism Spectrum Disorder. *Biological Psychiatry*. 2017;81(5):411-423. doi:10.1016/j.biopsych.2016.08.024.

40. Foster JA, McVey Neufeld K-A. Gut-brain axis: how the microbiome influences anxiety and depression. *Trends in Neurosciences*. 2013;36(5):305-312. doi:10.1016/j.tins.2013.01.005.

41. Simpson CA, Diaz-Arteche C, Eliby D, et al. The gut microbiota in anxiety and depression – A systematic review. *Clinical Psychology Review*. 2021;83:101943. doi:10.1016/j.cpr.2020.101943.

42. Cryan JF, O'Riordan KJ, Sandhu K, et al. The gut microbiome in neurological disorders. *The Lancet Neurology*. 2020;19(2):179-194. doi:10.1016/S1474-4422(19)30356-4.

43. Aho VTE, Houser MC, Pereira PAB, et al. Relationships of gut microbiota, short-chain fatty acids, inflammation, and the gut barrier in Parkinson's disease. *Molecular Neurodegeneration*. 2021;16(1):6. doi:10.1186/s13024-021-00427-6.

44. Lubomski M, Xu X, Holmes AJ, et al. The Gut Microbiome in Parkinson's Disease: A Longitudinal Study of the Impacts on Disease Progression and the Use of Device-Assisted Therapies. *Front Aging Neurosci*. 2022;14:875261. doi:10.3389/fnagi.2022.875261.

45. Kwon D, Zhang K, Paul KC, et al. Diet and the gut microbiome in patients with Parkinson's disease. *npj Parkinson's Disease*. 2024;10(1):89. doi:10.1038/s41531-024-00681-7.

46. Huang B, Chau SWH, Liu Y, et al. Gut microbiome dysbiosis across early Parkinson's disease, REM sleep behavior disorder and their first-degree relatives. *Nature Communications*. 2023;14(1):2501. doi:10.1038/s41467-023-38248-4.

47. Nishiwaki H, Ueyama J, Kashihara K, et al. Gut microbiota in dementia with Lewy bodies. *npj Parkinson's Disease*. 2022;8(1):169. doi:10.1038/s41531-022-00428-2.

48. Teigen LM, McCarter SJ, Ziegert Z, et al. Taxonomic intestinal microbiota differences in Lewy body spectrum disease and cohabitant controls. *Parkinsonism & Related Disorders*. 2024;129:107176. doi:10.1016/j.parkreldis.2024.107176.

49. Janda JM, Abbott SL. 16S rRNA gene sequencing for bacterial identification in the diagnostic laboratory: pluses, perils, and pitfalls. *J Clin Microbiol*. 2007;45(9):2761-4. doi:10.1128/jcm.01228-07.

50. Börnigen D, Morgan XC, Franzosa EA, et al. Functional profiling of the gut microbiome in disease-associated inflammation. *Genome Med*. 2013;5(7):65. doi:10.1186/gm469.

51. Sharon G, Sampson TR, Geschwind DH, et al. The Central Nervous System and the Gut Microbiome. *Cell*. 2016;167(4):915-932. doi:10.1016/j.cell.2016.10.027.

52. Strandwitz P. Neurotransmitter modulation by the gut microbiota. *Brain Res*. 2018;1693(Pt B):128-133. doi:10.1016/j.brainres.2018.03.015.

53. Parker A, Fonseca S, Carding SR. Gut microbes and metabolites as modulators of blood-brain barrier integrity and brain health. *Gut Microbes*. 2020;11(2):135-157. doi:10.1080/19490976.2019.1638722.

54. Erny D, Hrabě de Angelis AL, Prinz M. Communicating systems in the body: how microbiota and microglia cooperate. *Immunology*. 2017;150(1):7-15. doi:10.1111/imm.12645.

55. Lloyd-Price J, Abu-Ali G, Huttenhower C. The healthy human microbiome. *Genome medicine*. 2016;8(1):51. doi:10.1186/s13073-016-0307-y.

56. The Human Microbiome Project Consortium. Structure, function and diversity of the healthy human microbiome. *Nature*. 2012;486(7402):207-214. doi:10.1038/nature11234.

57. Turnbaugh PJ, Hamady M, Yatsunenko T, et al. A core gut microbiome in obese and lean twins. *Nature*. 2009;457(7228):480-484. doi:10.1038/nature07540.

58. Zhernakova A, Kurilshikov A, Bonder MJ, et al. Population-based metagenomics analysis reveals markers for gut microbiome composition and diversity. *Science*. 2016;352(6285):565-9. doi:10.1126/science.aad3369.

59. Rothschild D, Weissbrod O, Barkan E, et al. Environment dominates over host genetics in shaping human gut microbiota. *Nature*. 2018;555(7695):210-215. doi:10.1038/nature25973.

60. Tavalire HF, Christie DM, Leve LD, et al. Shared Environment and Genetics Shape the Gut Microbiome after Infant Adoption. *mBio*. 2021;12(2): e00548-21. doi:10.1128/mBio.00548-21.

61. Song SJ, Lauber C, Costello EK, et al. Cohabiting family members share microbiota with one another and with their dogs. *Elife*. 2013;2:e00458. doi:10.7554/eLife.00458.

62. Bolger AM, Lohse M, Usadel B. Trimmomatic: a flexible trimmer for Illumina sequence data. *Bioinformatics*. 2014;30(15):2114-20. doi:10.1093/bioinformatics/btu170.

63. Langmead B, Salzberg SL. Fast gapped-read alignment with Bowtie 2. *Nature Methods*. 2012;9(4):357-359. doi:10.1038/nmeth.1923.

64. Li H, Handsaker B, Wysoker A, et al. The Sequence Alignment/Map format and SAMtools. *Bioinformatics*. 2009;25(16):2078-9. doi:10.1093/bioinformatics/btp352.

65. Blanco-Míguez A, Beghini F, Cumbo F, et al. Extending and improving metagenomic taxonomic profiling with uncharacterized species using MetaPhlAn 4. *Nature Biotechnology*. 2023;41(11):1633-1644. doi:10.1038/s41587-023-01688-w.

66. Beghini F, McIver LJ, Blanco-Míguez A, et al. Integrating taxonomic, functional, and strain-level profiling of diverse microbial communities with bioBakery 3. *Elife*. 2021;10doi:10.7554/eLife.65088.

67. Abeles SR, Jones MB, Santiago-Rodriguez TM, et al. Microbial diversity in individuals and their household contacts following typical antibiotic courses. *Microbiome*. 2016;4(1):39. doi:10.1186/s40168-016-0187-9.

68. iMSMS Consortium. Gut microbiome of multiple sclerosis patients and paired household healthy controls reveal associations with disease risk and course. *Cell*. 2022;185(19):3467-3486.e16. doi:10.1016/j.cell.2022.08.021.

69. Huang Z, Wang C, Huang Q, et al. Hungatella hathewayi impairs the sensitivity of colorectal cancer cells to 5-FU through decreasing CDX2 expression. *Human Cell*. 2023;36(6):2055-2065. doi:10.1007/s13577-023-00938-y.

70. Chan C, Leung T, Choi K, et al. Association of early-life gut microbiome and lifestyle factors in the development of eczema in Hong Kong infants. *Experimental Dermatology*. 2021;30:859-864. doi:10.1111/exd.14280.

71. Rawat PS, Li Y, Zhang W, et al. *Hungatella hathewayi*, an Efficient Glycosaminoglycan-Degrading Firmicutes from Human Gut and Its Chondroitin ABC Exolyase with High Activity and Broad Substrate Specificity. *Appl Environ Microbiol*. 2022;88(22):e0154622. doi:10.1128/aem.01546-22.

72. Francis KL, Zheng HB, Suskind DL, et al. Characterizing the human intestinal chondroitin sulfate glycosaminoglycan sulfation signature in inflammatory bowel disease. *Scientific Reports*. 2024;14(1):11839. doi:10.1038/s41598-024-60959-x.

73. Noda K, Atale N, Al-Zahrani A, et al. Heparanase-induced endothelial glycocalyx degradation exacerbates lung ischemia/reperfusion injury in male mice. *Physiol Rep*. 2024;12(20):e70113. doi:10.14814/phy2.70113.

74. Hurst RE, Van Gordon S, Tyler K, et al. In the absence of overt urothelial damage, chondroitinase ABC digestion of the GAG layer increases bladder permeability in ovariectomized female rats. *Am J Physiol Renal Physiol*. 2016;310(10):F1074-80. doi:10.1152/ajprenal.00566.2015.

75. Shoubridge AP, Carpenter L, Flynn E, et al. Severe Cognitive Decline in Long-term Care Is Related to Gut Microbiome Production of Metabolites Involved in Neurotransmission, Immunomodulation, and Autophagy. *J Gerontol A Biol Sci Med Sci*. 2025;80(7):glaf053. doi: 10.1093/gerona/glaf053.

76. Chen J, Wright K, Davis JM, et al. An expansion of rare lineage intestinal microbes characterizes rheumatoid arthritis. *Genome Medicine*. 2016;8(1):43. doi:10.1186/s13073-016-0299-7.

77. Song L, Sun Q, Zheng H, et al. Roseburia hominis Alleviates Neuroinflammation via Short-Chain Fatty Acids through Histone Deacetylase Inhibition. *Mol Nutr Food Res*. 2022;66(18):e2200164. doi:10.1002/mnfr.202200164.

78. Mukherjee A, Lordan C, Ross RP, et al. Gut microbes from the phylogenetically diverse genus Eubacterium and their various contributions to gut health. *Gut Microbes*. 2020;12(1):1802866. doi:10.1080/19490976.2020.1802866.

79. Bui TP, Shetty SA, Lagkouvardos I, et al. Comparative genomics and physiology of the butyrate-producing bacterium Intestinimonas butyriciproducens. *Environ Microbiol Rep*. 2016;8(6):1024-1037. doi:10.1111/1758-2229.12483.

80. Cheng J, Hu J, Geng F, Nie S. Bacteroides utilization for dietary polysaccharides and their beneficial effects on gut health. *Food Science and Human Wellness*. 2022;11(5):1101-1110. doi:10.1016/j.fshw.2022.04.002.

81. Rodriguez-Castaño GP, Dorris MR, Liu X, et al. *Bacteroides thetaiotaomicron* Starch Utilization Promotes Quercetin Degradation and Butyrate Production by *Eubacterium ramulus*. Original Research. *Frontiers in Microbiology*. 2019;10:1145. doi: 10.3389/fmicb.2019.01145.

82. Rios-Covian D, Salazar N, Gueimonde M, et al. Shaping the Metabolism of Intestinal Bacteroides Population through Diet to Improve Human Health. Opinion. *Frontiers in Microbiology*. 2017; 8:376. doi:10.3389/fmicb.2017.00376.

83. Deleu S, Machiels K, Raes J, et al. Short chain fatty acids and its producing organisms: An overlooked therapy for IBD? *eBioMedicine*. 2021;66. doi:10.1016/j.ebiom.2021.103293.

84. Facchin S, Bertin L, Bonazzi E, et al. Short-Chain Fatty Acids and Human Health: From Metabolic Pathways to Current Therapeutic Implications. *Life*. 2024;14(5):559. doi:10.3390/life14050559

85. Cryan JF, Dinan TG. Mind-altering microorganisms: the impact of the gut microbiota on brain and behaviour. *Nat Rev Neurosci*. 2012;13(10):701-12. doi:10.1038/nrn3346.

86. Sherwin E, Rea K, Dinan TG, et al. A gut (microbiome) feeling about the brain. *Curr Opin Gastroenterol*. 2016;32(2):96-102. doi:10.1097/mog.0000000000000244.

87. Hsiao EY, McBride SW, Hsien S, et al. Microbiota modulate behavioral and physiological abnormalities associated with neurodevelopmental disorders. *Cell*. 2013;155(7):1451-63. doi:10.1016/j.cell.2013.11.024.

88. Flint HJ, Scott KP, Duncan SH, et al. Microbial degradation of complex carbohydrates in the gut. *Gut Microbes*. 2012;3(4):289-306. doi:10.4161/gmic.19897.

89. Cockburn DW, Koropatkin NM. Polysaccharide Degradation by the Intestinal Microbiota and Its Influence on Human Health and Disease. *J Mol Biol*. 2016;428(16):3230-3252. doi:10.1016/j.jmb.2016.06.021.

90. Louis P, Flint HJ. Formation of propionate and butyrate by the human colonic microbiota. *Environ Microbiol*. 2017;19(1):29-41. doi:10.1111/1462-2920.13589.

91. Waniewski RA, Martin DL. Preferential utilization of acetate by astrocytes is attributable to transport. *J Neurosci*. 1998;18(14):5225-33. doi:10.1523/jneurosci.18-14-05225.1998.

92. Frost G, Sleeth ML, Sahuri-Arisoylu M, et al. The short-chain fatty acid acetate reduces appetite via a central homeostatic mechanism. *Nature Communications*. 2014;5(1):3611. doi:10.1038/ncomms4611.

93. Soliman ML, Rosenberger TA. Acetate supplementation increases brain histone acetylation and inhibits histone deacetylase activity and expression. *Mol Cell Biochem*. 2011;352(1-2):173-80. doi:10.1007/s11010-011-0751-3.

94. Mews P, Donahue G, Drake AM, et al. Acetyl-CoA synthetase regulates histone acetylation and hippocampal memory. *Nature*. 2017;546(7658):381-386. doi:10.1038/nature22405.

95. Meldrum BS. Glutamate as a neurotransmitter in the brain: review of physiology and pathology. *J Nutr*. 2000;130(4S Suppl):1007s-15s. doi:10.1093/jn/130.4.1007S.

96. Lanctôt KL, Herrmann N, Mazzotta P. Role of serotonin in the behavioral and psychological symptoms of dementia. *J Neuropsychiatry Clin Neurosci*. 2001;13(1):5-21. doi:10.1176/jnp.13.1.5.

97. Braga JD, Thongngam M, Kumrungsee T. Gamma-aminobutyric acid as a potential postbiotic mediator in the gut-brain axis. *npj Science of Food*. 2024;8(1):16. doi:10.1038/s41538-024-00253-2.

98. Marzouk NH, Rashwan HH, El-Hadidi M, et al. Proinflammatory and GABA eating bacteria in Parkinson's disease gut microbiome from a meta-analysis perspective. *npj Parkinson's Disease*. 2025;11(1):145. doi:10.1038/s41531-025-00950-z.

99. Wallen ZD, Demirkan A, Twa G, et al. Metagenomics of Parkinson's disease implicates the gut microbiome in multiple disease mechanisms. *Nat Commun*. 2022;13(1):6958. doi:10.1038/s41467-022-34667-x.

100. Zhong HJ, Wang SQ, Zhang RX, et al. Supplementation with high-GABA-producing Lactobacillus plantarum L5 ameliorates essential tremor triggered by decreased gut bacteria-derived GABA. *Translational Neurodegeneration*. 2023;12(1):58. doi:10.1186/s40035-023-00391-9.

101. Sun H, Zhao F, Liu Y, et al. Probiotics synergized with conventional regimen in managing Parkinson's disease. *NPJ Parkinsons Dis*. 2022;8(1):62. doi:10.1038/s41531-022-00327-6.

102. Kneidinger B, Marolda C, Graninger M, et al. Biosynthesis pathway of ADP-L-glycero-beta-D-manno-heptose in Escherichia coli. *J Bacteriol*. 2002;184(2):363-9. doi:10.1128/jb.184.2.363-369.2002.

103. Whitfield C, Williams DM, Kelly SD. Lipopolysaccharide O-antigens-bacterial glycans made to measure. *J Biol Chem*. 2020;295(31):10593-10609. doi:10.1074/jbc.REV120.009402.

104. Bertani B, Ruiz N. Function and Biogenesis of Lipopolysaccharides. *EcoSal Plus*. Aug 2018;8(1). doi:10.1128/ecosalplus.ESP-0001-2018

105. Raetz CR, Whitfield C. Lipopolysaccharide endotoxins. *Annu Rev Biochem*. 2002;71:635-700. doi:10.1146/annurev.biochem.71.110601.135414.

106. Nighot M, Al-Sadi R, Guo S, et al. Lipopolysaccharide-Induced Increase in Intestinal Epithelial Tight Permeability Is Mediated by Toll-Like Receptor 4/Myeloid Differentiation Primary Response 88 (MyD88) Activation of Myosin Light Chain Kinase Expression. *The American Journal of Pathology*. 2017;187(12):2698-2710. doi:10.1016/j.ajpath.2017.08.005.

107. Guo S, Al-Sadi R, Said HM, et al. Lipopolysaccharide Causes an Increase in Intestinal Tight Junction Permeability in Vitro and in Vivo by Inducing Enterocyte Membrane Expression and Localization of TLR-4 and CD14. *The American Journal of Pathology*. 2013;182(2):375-387. doi:10.1016/j.ajpath.2012.10.014.

108. Guo S, Nighot M, Al-Sadi R, et al. Lipopolysaccharide Regulation of Intestinal Tight Junction Permeability Is Mediated by TLR4 Signal Transduction Pathway Activation of FAK and MyD88. *J Immunol*. 2015;195(10):4999-5010. doi:10.4049/jimmunol.1402598.

109. van Kessel SP, El Aidy S. Bacterial Metabolites Mirror Altered Gut Microbiota Composition in Patients with Parkinson's Disease. *J Parkinsons Dis*. 2019;9(s2):S359-s370. doi:10.3233/jpd-191780.

110. Bhattacharyya D, Mohite GM, Krishnamoorthy J, et al. Lipopolysaccharide from Gut Microbiota Modulates α-Synuclein Aggregation and Alters Its Biological Function. *ACS Chem Neurosci*. 2019;10(5):2229-2236. doi:10.1021/acschemneuro.8b00733.

111. Bhattacharyya D, Bhunia A. Gut-Brain axis in Parkinson's disease etiology: The role of lipopolysaccharide *Chemistry and Physics of Lipids*. 2021;235:105029. doi:10.1016/j.chemphyslip.2020.105029.

112. Deng I, Corrigan F, Zhai G, et al. Lipopolysaccharide animal models of Parkinson's disease: Recent progress and relevance to clinical disease. *Brain, Behavior, & Immunity - Health*. 2020;4:100060. doi:10.1016/j.bbih.2020.100060.

113. Block ML, Zecca L, Hong JS. Microglia-mediated neurotoxicity: uncovering the molecular mechanisms. *Nature Reviews Neuroscience*. 2007;8(1):57-69. doi:10.1038/nrn2038.

114. Rosadini CV, Kagan JC. Early innate immune responses to bacterial LPS. *Current Opinion in Immunology*. 2017;44:14-19. doi:10.1016/j.coi.2016.10.005.

115. Qin L, Wu X, Block ML, et al. Systemic LPS causes chronic neuroinflammation and progressive neurodegeneration. *Glia*. 2007;55(5):453-62. doi:10.1002/glia.20467.

116. Gao HM, Hong JS, Zhang W, et al. Synergistic dopaminergic neurotoxicity of the pesticide rotenone and inflammogen lipopolysaccharide: relevance to the etiology of Parkinson's disease. *J Neurosci*. 2003;23(4):1228-36. doi:10.1523/jneurosci.23-04-01228.2003.

117. Castaño A, Herrera AJ, Cano J, et al. Lipopolysaccharide intranigral injection induces inflammatory reaction and damage in nigrostriatal dopaminergic system. *J Neurochem*. 1998;70(4):1584-92. doi:10.1046/j.1471-4159.1998.70041584.x.

118. Rajilić-Stojanović M, de Vos WM. The first 1000 cultured species of the human gastrointestinal microbiota. *FEMS Microbiol Rev*. 2014;38(5):996-1047. doi:10.1111/1574-6976.12075.

119. Kropp C, Tambosco K, Chadi S, et al. *Christensenella minuta* protects and restores intestinal barrier in a colitis mouse model by regulating inflammation. *npj Biofilms and Microbiomes*. 2024;10(1):88. doi:10.1038/s41522-024-00540-6.

120. Kropp C, Le Corf K, Relizani K, et al. The Keystone commensal bacterium *Christensenella minuta* DSM 22607 displays anti-inflammatory properties both in vitro and in vivo. *Scientific Reports*. 2021;11(1):11494. doi:10.1038/s41598-021-90885-1.

121. Borrelli L, Coretti L, Dipineto L, et al. Insect-based diet, a promising nutritional source, modulates gut microbiota composition and SCFAs production in laying hens. *Scientific reports*. 2017;7(1):16269. doi:10.1038/s41598-017-16560-6.

122. Singh V, Lee G, Son H, et al. Butyrate producers, "The Sentinel of Gut": Their intestinal significance with and beyond butyrate, and prospective use as microbial therapeutics. *Front Microbiol*. 2022;13:1103836. doi:10.3389/fmicb.2022.1103836.

123. Hertz L, Peng L, Dienel GA. Energy metabolism in astrocytes: high rate of oxidative metabolism and spatiotemporal dependence on glycolysis/glycogenolysis. *J Cereb Blood Flow Metab*. 2007;27(2):219-49. doi:10.1038/sj.jcbfm.9600343.

124. Bak LK, Schousboe A, Waagepetersen HS. The glutamate/GABA-glutamine cycle: aspects of transport, neurotransmitter homeostasis and ammonia transfer. *J Neurochem*. 2006;98(3):641-53. doi:10.1111/j.1471-4159.2006.03913.x.

125. Hertz L, Dringen R, Schousboe A, Robinson SR. Astrocytes: glutamate producers for neurons. *J Neurosci Res*. 1999;57(4):417-28. doi:10.1002/(SICI)1097-4547(19990815)57:4<417::AID-JNR1>3.0.CO;2-N.

126. Bak LK, Sickmann HM, Schousboe A, et al. Activity of the lactate-alanine shuttle is independent of glutamate-glutamine cycle activity in cerebellar neuronal-astrocytic cultures. *J Neurosci Res*. 2005;79(1-2):88-96. doi:10.1002/jnr.20319.

127. Pokusaeva K, Fitzgerald GF, van Sinderen D. Carbohydrate metabolism in Bifidobacteria. *Genes Nutr*. 2011;6(3):285-306. doi:10.1007/s12263-010-0206-6.

128. Vries Wd, Stouthamer AH. Pathway of Glucose Fermentation in Relation to the Taxonomy of Bifidobacteria. *Journal of Bacteriology*. 1967;93(2):574-576. doi:doi:10.1128/jb.93.2.574-576.1967.

129. Duncan SH, Louis P, Flint HJ. Lactate-utilizing bacteria, isolated from human feces, that produce butyrate as a major fermentation product. *Appl Environ Microbiol*. 2004;70(10):5810-7. doi:10.1128/aem.70.10.5810-5817.2004.

130. Belenguer A, Duncan SH, Holtrop G, et al. Impact of pH on lactate formation and utilization by human fecal microbial communities. *Appl Environ Microbiol*. 2007;73(20):6526-33. doi:10.1128/aem.00508-07.

131. LeBlanc JG, Chain F, Martín R, et al. Beneficial effects on host energy metabolism of short-chain fatty acids and vitamins produced by commensal and probiotic bacteria. *Microb Cell Fact*. 2017;16(1):79. doi:10.1186/s12934-017-0691-z.

132. Voevodskaya O, Poulakis K, Sundgren P, et al. Brain myoinositol as a potential marker of amyloid-related pathology: A longitudinal study. *Neurology*. 2019;92(5):e395-e405. doi:10.1212/wnl.0000000000006852.

133. Murray ME, Przybelski SA, Lesnick TG, et al. Early Alzheimer's disease neuropathology detected by proton MR spectroscopy. *J Neurosci*. 2014;34(49):16247-55. doi:10.1523/jneurosci.2027-14.2014.

134. Heaver SL, Le HH, Tang P, et al. Characterization of inositol lipid metabolism in gut-associated Bacteroidetes. *Nature Microbiology*. 2022;7(7):986-1000. doi:10.1038/s41564-022-01152-6.

135. Jessen H, Bui TPN. Metabolism of inositol derivatives by the gut microbiome. *Gut Microbes*. 2025;17(1):2564765. doi:10.1080/19490976.2025.2564765.

136. Zeng Z, Dank A, Smid EJ, et al. Bacterial microcompartments in food-related microbes. *Current Opinion in Food Science*. 2022;43:128-135. doi:10.1016/j.cofs.2021.11.011.

137. Saxena R, Anand P, Saran S, et al. Microbial production and applications of 1,2-propanediol. *Indian journal of microbiology*. 2010;50:2-11. doi:10.1007/s12088-010-0017-x.

138. Reichardt N, Duncan SH, Young P, et al. Phylogenetic distribution of three pathways for propionate production within the human gut microbiota. *The ISME Journal*. 2014;8(6):1323-1335. doi:10.1038/ismej.2014.14.

139. Fusco W, Lorenzo MB, Cintoni M, et al. Short-Chain Fatty-Acid-Producing Bacteria: Key Components of the Human Gut Microbiota. *Nutrients*. 2023;15(9). doi:10.3390/nu15092211.

140. Schober I, Koblitz J, Sardà Carbasse J, et al. BacDive in 2025: the core database for prokaryotic strain data. *Nucleic Acids Research*. 2024;53(D1):D748-D756. doi:10.1093/nar/gkae959.